

# Data-driven Predictive Control for a Class of Uncertain Control-Affine Systems

Dan Li<sup>1</sup>, Dariush Fooladivanda<sup>1</sup> and Sonia Martínez<sup>1</sup>

## Abstract

This paper studies a data-driven predictive control for a class of control-affine systems which is subject to uncertainty. With the accessibility to finite sample measurements of the uncertain variables, we aim to find controls which are feasible and provide superior performance guarantees with high probability. This results into the formulation of a stochastic optimization problem (P), which is intractable due to the unknown distribution of the uncertainty variables. By developing a distributionally robust optimization framework, we present an equivalent and yet tractable reformulation of (P). Further, we propose an efficient algorithm that provides online suboptimal data-driven solutions and guarantees performance with high probability. To illustrate the effectiveness of the proposed approach, we consider a highway speed-limit control problem. We then develop a set of data-driven speed controls that allow us to prevent traffic congestion with high probability. Finally, we employ the resulting control method on a traffic simulator to illustrate the effectiveness of this approach numerically.

## I. INTRODUCTION

Uncertainty is ubiquitous in real-world complex systems, including financial markets [1], human-robot mixed systems [2]–[4] or transportation networks [5]–[7]. Thanks to new advances in computation, communication, and innovative infrastructure, large amounts of data have become widely accessible, which can help reduce uncertainty in system design and control [2]. Stochastic *Model Predictive Control* (MPC) is a general framework that can handle broad types of system uncertainty in a tractable manner [8]–[12]. In general, the effectiveness of MPC depends on the particular problem of interest, roughly classified according to three criterion: 1) the class of systems to be controlled, e.g., linear [13], [14] or nonlinear systems [15]–[18]; 2) the way uncertainty is handled, e.g., stochastic [19]–[21] or bounded uncertainty [22]; and 3) the solution method, e.g., quadratic programming [11], stochastic programming [15], [23], or nonconvex optimization [9], [24]. In practice, system performance guarantees typically require large amounts of data processing which, for online settings such as MPC, may become specially challenging.

Motivated by the need of developing finite-data-driven predictive control methods, we consider the application of a *Distributionally Robust Optimization* (DRO) framework to a class of MPC problems. DRO has attracted recent attention due to its finite-sample performance guarantees [25], [26], problem tractability via Wasserstein ambiguity sets [27]–[29], its distributed formulation [30], [31] and online implementation [32]. These characteristics provide a novel mechanism to deal with uncertainty in MPC, while allowing for the tractability of the associated nonconvex optimization problems. In practice, the efficacy of the DRO framework depends on the explicit system structure. Here, our proposed approach applies to a problem class whose

\*This research was developed with funding from ONR contract N00014-19-1-2471 and DARPA (Lagrange) contract N660011824027. The views, opinions and/or findings expressed are those of the author and should not be interpreted as representing the official views or policies of the Department of Defense or the U.S. Government.

<sup>1</sup>D. Li, D. Fooladivanda and S. Martínez are with the Department of Mechanical and Aerospace Engineering, University of California San Diego, La Jolla, CA 92092, USA [lidan@ucsd.edu](mailto:lidan@ucsd.edu); [dfooladivanda@ucsd.edu](mailto:dfooladivanda@ucsd.edu); [soniamd@ucsd.edu](mailto:soniamd@ucsd.edu)

dynamics can be nonlinear, but affine both in control and states, and constraints can be linear or bi-linear.

For illustration purposes, we apply our solution method to toy examples related to highway speed-limit control, focusing our discussion on its performance with respect to uncertainty. As the highway congestion significantly affects system operations [33], a variety of congestion mitigation strategies have been proposed, including those based on optimization [34]–[36], logic-based control [37], extremum seeking control [38], and autonomous-vehicle scheduling [39]. More recently, *Speed-Limit Control* has been proposed as an effective mechanism in transportation [40], [41]. In particular, optimization-based speed-limit control has successfully demonstrated the containment of traffic congestion. For example, [42] proposed a discrete macroscopic second-order model, METANET, and used it in optimization problems for speed limit. However, at that time, the robustness analysis with respect to the system uncertainty was absent. Later in [43], a linear model predictive control of speed limit was developed for congestion mitigation. This work exploited the celebrated *Cell Transmission Model* (CTM) [44] or its extension for inhomogeneous traffic, the *Link Transmission Model* (LTM), to capture the deterministic distribution of traffic densities along a highway, and the dynamic properties of highways are characterized for congestion reduction, with relative low online computational costs. In addition, [45] proposed a scenario-based optimization to account for the bounded uncertainty of transportation systems. However, an explicit treatment of the system uncertainty, such as unknown drivers actions, vehicle arrival and departures, and as well as random events that happen on highways, are yet to be fully explored.

With increasing accessibility of real-time traffic data [46], [47] for uncertainty reduction, congestion mitigation and traffic control under uncertainty can become practical. As a first step into developing a novel data-driven traffic control methods, we consider a problem related to highway transportation, formulated by way of an extended CTM and controlled by speed limit, and customize our proposed framework with the following question in mind: *Can we find an efficient approach for the computation of data-driven controls with guarantees on congestion elimination?* We would like to note that, while the particular problem we look at is inspired by traffic-congestion mitigation, the main emphasis of this work is on the solution approach.

*Statement of Contributions.* This work presents the following contributions: 1) We first provide a general framework for data-driven predictive control under uncertainty. To demonstrate our approach explicitly, we consider a problem inspired by highway speed-limit control which extends the CTM to account for random events (due to drivers actions) as well as vehicle arrival and departures. This provides an analytical framework and a stochastic optimization problem formulation for the computation of speed limit using the available flow measurements (in Section II). 2) We propose an optimization-based data-driven control approach that extends DRO to account for system dynamics. The resulting approach guarantees congestion elimination with high probability, using only finite flow measurements (in Section III). 3) As the proposed data-driven optimization problem is infinite dimensional and intractable, we propose an equivalent reformulation that reduces the proposed problem into a finite-dimensional optimization problem (in Section III). 4) Yet this problem is non-convex and difficult to solve, so we find an equivalent reformulation via a binary representation technique, and propose a computationally efficient algorithm to provide online sub-optimal speed limits that ensure congestion elimination and guarantee of highway throughput with high probability (in Section V). 5) We propose in Section VI an optimization tool to analyze the performance of the proposed algorithm offline. This tool is developed via a second-order cone relaxation technique and we show that, under mild conditions, the resulting Mixed-Integer Second-Order Cone Problem (MISOCP) is exact, and can be handled by commercial solvers. 6) We numerically demonstrate the effectiveness of

our data-driven approach with performance guarantees, in Section VII and VIII. We claim that the proposed approach is suitable for problems which are subject to control-affine constraints.

A preliminary study of this work appeared in [7], however the differences are the following: This work 1) considers a general optimization framework, 2) demonstrates a detailed procedure of the proposed integer-solution search algorithm, 3) provides an exact MISOCP relaxation as a tool for solution analysis, and 4) studies the effectiveness of the proposed approach in application.

*Notation:* See the footnote<sup>1</sup> for basic notations of this work.

## II. PROBLEM FORMULATION

We first present our data-driven predictive control approach in a general setting with the main goal of control design employing a finite data set. We then focus on an one-way highway speed-limit control as an application. This problem leverages a traffic model based on the Lighthill-Whitham-Richards (LWR) discretization [48]–[51]. Finally, we adapt the proposed predictive control approach for our control problem, resulting into a stochastic optimization problem that can be used to find speed limits with performance guarantees.

### A. General Optimization Framework for Stochastic MPC

The goal of the proposed framework is to address system uncertainty explicitly and find a control law which satisfies system constraints and optimizes the expected objective in uncertainty. To achieve this, let us denote by  $t \in \mathbb{N}$ ,  $x(t) \in \mathbb{R}^n$  and  $u(t) \in \mathbb{R}^m$  the time, system state and control at time  $t$ , respectively. We consider the control law  $u$  to be solutions of the following  $T$ -long receding-horizon stochastic predictive control problem:

$$\begin{aligned}
 (\mathbf{P}) \quad & \sup_u \mathbb{E}_{\mathbb{P}(u)} [\ell(u, x)], \\
 & \text{s. t. } x \sim \mathbb{P}(u) \text{ characterized by} \\
 & x(t+1) = F(x(t), u(t), \xi(t)), \quad t = 0, 1, \dots, T-1, \\
 & x \in \mathcal{Z}(u), \quad u \in \mathcal{U}, \quad \xi \sim \mathbb{P}_\xi,
 \end{aligned}$$

where  $u$  is a concatenated variable of  $u(0), u(1), \dots, u(T-1)$  and  $x$  is that of those  $x(t)$ . Notice that  $x$  is a stochastic process and we denote by  $\mathbb{P}(u)$  the distribution of  $x$  given  $u$ . The objective is to maximize the expectation of a given reward function  $\ell : \mathbb{R}^{mT} \times \mathbb{R}^{nT} \rightarrow \mathbb{R}$  taken under

<sup>1</sup>Let  $\mathbb{R}^{m \times n}$  denote the  $m \times n$ -dimensional real vector space, and let  $\mathbf{1}_m$  and  $\mathbf{0}_m$  denote the column vectors  $(1, \dots, 1)^\top \in \mathbb{R}^m$  and  $(0, \dots, 0)^\top \in \mathbb{R}^m$ , respectively. For any vector  $x \in \mathbb{R}^m$ , let us denote  $x \geq \mathbf{0}_m$  if all the entries are nonnegative. Any letter  $x$  may have appended the following indices and arguments: it may have the subscript  $x_e$  with  $e \in \mathbb{N}$ , the argument  $x_e(t)$  with  $t \in \mathbb{N}$ , and finally a superscript  $l \in \mathbb{N}$  as in  $x_e^{(l)}(t)$ . Given a finite number of elements  $x_e^{(l)}(t) \in \mathbb{R}$  where  $e, t, l \in \mathbb{N}$ , we define vectors  $x^{(l)}(t) := (x_1^{(l)}(t), x_2^{(l)}(t), \dots)$ ,  $x^{(l)} := (x^{(l)}(1), x^{(l)}(2), \dots)$ , and  $x := (x^{(1)}, x^{(2)}, \dots)$ . Let  $\langle x, y \rangle$  and  $x \circ y$  denote the inner and component-wise products of vectors  $x, y \in \mathbb{R}^m$ , respectively. The component-wise square of vector  $x \in \mathbb{R}^m$  is denoted by  $x^2 := x \circ x$ . In addition, let  $x \otimes y$  denote the Kronecker product of vectors  $x, y$  with arbitrary dimension. Let  $\|x\|$  denote the 1-norm of  $x \in \mathbb{R}^m$ , and let  $\|x\|_* := \sup_{\|z\| \leq 1} \langle z, x \rangle$  denote the corresponding dual norm. Notice that  $\|x\|_{**} = \|x\|$ . **Optimization theory:** Consider a bounded function  $f : X \rightarrow \mathbb{R}$  where  $X \subseteq \mathbb{R}^n$ . The function  $f$  is lower semi-continuous on  $X$  if  $f(x) \leq \liminf_{y \rightarrow x} f(y)$  for all  $x \in X$ . Similarly, the function  $f$  is lower semi-continuous on  $X$  if and only if its sublevel sets  $\{x \in X \mid f(x) \leq \gamma\}$  are closed for each  $\gamma \in \mathbb{R}$ . We let  $f^* : X \rightarrow \mathbb{R} \cup \{+\infty\}$  denote the convex conjugate of  $f$ , which is defined as  $f^*(x) := \sup_{y \in X} \langle x, y \rangle - f(y)$ . Further, the infimal convolution of two functions  $f$  and  $g$  on  $X$  is defined as  $(f \square g)(x) := \inf_{y \in X} f(x-y) + g(y)$ . If  $f$  and  $g$  are bounded, convex, and lower semi-continuous functions on  $X$ , we will have  $(f+g)^* = (f^* \square g^*)$ .

Consider a subset  $A \subset X$ , and let  $\chi_A : X \rightarrow \mathbb{R} \cup \{+\infty\}$  denote the characteristic function of  $A$ , i.e.,  $\chi_A(x)$  is equal to 0 if and only if  $x \in A$  and  $+\infty$  otherwise. In addition, let  $\sigma_A : X \rightarrow \mathbb{R}$  denote the support function of  $A$ , which is defined as  $\sigma_A(x) := \sup_{y \in A} \langle x, y \rangle$ . Notice that  $\chi_A$  is lower semi-continuous if and only if  $A$  is closed, and that  $\sigma_A(x) = [\chi_A]^*(x)$  for all  $x \in X$ .

$\mathbb{P}(u)$ . We denote by  $F : \mathbb{R}^n \times \mathbb{R}^m \times \mathbb{R}^d \rightarrow \mathbb{R}^n$  the given system dynamics where  $\xi$  represents the uncertainty. We assume that the process  $x$  is constrained in a given set  $\mathcal{Z}(u)$  and so does  $u$  in  $\mathcal{U}$ . We denote by  $\mathbb{P}_\xi$  the unknown distribution of the uncertainty process.

Due to the unknown  $\mathbb{P}_\xi$ , Problem **(P)** cannot be solved exactly. To find a control law that solves **(P)**, we propose a distributionally robust optimization (DRO) framework. By means of this, we will employ a finite set of realizations or samples of the random variables  $\xi$  to approximate the unknown distribution and compute a set of feasible  $u$ . The main appeal of this robust method is that it can provide *out-of-sample* probabilistic guarantees of performance [26]. In particular, at each  $t$ , let us assume that  $N$  samples of  $x(0)$  and  $\xi := (\xi(0), \dots, \xi(T-1))$  are accessible. Under some mild conditions on these samples, we will show in Section III that a tractable optimization-based function  $J(u)$  can be constructed using those state and uncertainty samples. The function  $J(u)$  is a surrogate objective of **(P)** which accounts for the system dynamics as well as constraints on the states. In addition, given a confidence value  $\beta \in (0, 1)$ , we provide the *out-of-sample* performance guarantee in the sense that the probability of the true objective function in **(P)** being greater than  $J(u)$  is greater than  $1 - \beta$ . In other words, we have

$$\text{Prob}^N (\mathbb{E}_{\mathbb{P}(u)} [\ell(u, x)] \geq J(u)) \geq 1 - \beta,$$

where  $\text{Prob}^N$  is the product probability over  $N$  sample trajectories of the system. Thus, with high probability, the choice of samples to approximate the problem will provide a minimum lower value for the original problem. As Problem **(P)** needs to be solved in a moving horizon fashion, the surrogate functions  $J(u)$  is optimized similarly, as in Algorithm 1. Notice that, the functions  $J(u)$  depend on samples as well as the system structure, and the solution to  $J(u)$  is nontrivial.

---

**Algorithm 1** Data-driven predictive control with guarantees

---

- 1: Initialize  $t = 0$
  - 2: **while** True **do**
  - 3:     Take  $N$  measurements  $x^{(l)}(t)$  and  $\xi^{(l)}$ ,  $l = 1, \dots, N$
  - 4:     Adapt an approach to optimize  $J(u)$  over  $u$
  - 5:     Apply performance-guaranteed  $u$  to the system
  - 6:      $t \leftarrow t + 1$
  - 7: **end while**
- 

To enable the proposed tractable optimization method for  $J(u)$  as in Section V, we assume the following system structures.

**Assumption II.1 (Control-and-state-affine systems with bi-linear constraints)** *The system dynamics  $F(x, u, \xi)$  is continuous, affine in  $x$  and affine in  $u$ . In addition, the set  $\mathcal{Z}(u)$  is composed of constraints which are linear and bi-linear in  $(x, u)$ . And the set  $\mathcal{U}$  is a finite set.*

Assumption II.1 covers a wide class of dynamical systems, including linear systems and bi-linear systems. Furthermore, with a minor modification of the proposed reformulation techniques in Section IV, the proposed solution method can be extended to control-affine systems. We leave the extension as the future work. Next, we consider a traffic speed-limit control problem and design a set of speed controls using the proposed framework.



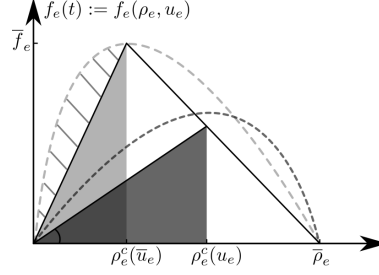


Fig. 2: Flow rate as a function of traffic density of edge  $e$  for two speed limits  $\bar{u}_e$  and  $u_e$  such that  $\bar{u}_e \geq u_e$ . The two nonlinear curves are the fundamental diagrams corresponding to each speed limit, while the straight lines are piece-wise linear approximations of these. The slope of linear approximations at the origin represents the speed limits  $\bar{u}_e$  and  $u_e$ , respectively. The light and dark shaded region guarantees no congestion of edge  $e$  under speed limit  $\bar{u}_e$  and  $u_e$ , respectively. (That is, under speed limit  $u_e$ , a density such that  $\rho_e(t) \leq \rho_e^c(u_e)$ , for all  $t$ , guarantees no congestion.) The slashed area reflects the compliance of drivers with speed limit  $\bar{u}_e$ . A higher compliance of drivers results in a smaller area.

attains its maximum value,  $\bar{f}_e$ , is called the *critical density*,  $\rho_e^c$ . The density at which the traffic flow is zero is the traffic jam density  $\bar{\rho}_e$ . The traffic flow is an increasing function of  $\rho_e$  on  $(0, \rho_e^c)$ , and a strictly decreasing function of  $\rho_e$  on  $(\rho_e^c, \bar{\rho}_e)$ .

How speed limits affect the fundamental diagram has been a subject of debate [40], [41]. Following [40], we will assume that in the presence of speed limits, the flow rate and traffic density still hold a similar relationship, however the critical density will be a function of the velocity limit  $u_e(t)$ . Let  $\bar{u}_e$  be the free flow velocity corresponding to a maximum value of flow under no speed limits.<sup>2</sup> A comparison of two fundamental diagrams with constant speed limits  $\bar{u}_e$  and  $u_e$  are shown in Fig. 2. Notice that the reduction of the speed limit from  $\bar{u}_e$  to  $u_e$  increases the critical density and decreases the maximal flow rate on edge  $e$ .

To model the fundamental diagram in the presence of speed limits, consider edge  $e \in \mathcal{E}$ , and let  $\rho_e^c(u_e(t))$  denote the critical density of edge  $e$  at speed limit  $u_e(t)$ . That is, the critical density  $\rho_e^c(u_e(t))$  determines the traffic density at which the maximum edge flow  $f_e(t)$  is achievable. Given speed limit  $u_e(t)$ , we will work with an approximation of the fundamental diagram of edge  $e \in \mathcal{E}$  given as follows

$$f_e(t) = \begin{cases} u_e(t)\rho_e(t), & \text{if } \rho_e(t) \leq \rho_e^c(u_e(t)), \\ \tau_e \bar{u}_e (\bar{\rho}_e - \rho_e(t)), & \text{otherwise,} \end{cases} \quad (1)$$

with<sup>3</sup>

$$\rho_e^c(u_e(t)) := (\tau_e \bar{\rho}_e \bar{u}_e) / (\tau_e \bar{u}_e + u_e(t)),$$

where the parameter  $\tau_e := \bar{f}_e / (\bar{u}_e \bar{\rho}_e - \bar{f}_e)$ . To illustrate this, we refer the reader to Fig. 2.

Each segment  $e$  is congested when its density is higher than its critical density (see, e.g., [41], [54]). Since critical densities are determined by speed limits, we select the speed limits such that the following constraint is satisfied at all time slots  $t \in \mathcal{T}$

$$0 \leq \rho_e(t) \leq \rho_e^c(u_e(t)), \quad \forall e \in \mathcal{E}. \quad (2)$$

<sup>2</sup>Given drivers behavior  $\bar{s}_e$ , the value  $\bar{u}_e = \max_{\rho_e} \bar{s}_e(\rho_e)$ ,  $\bar{\rho}_e$  admits  $\bar{s}_e(\bar{\rho}_e) = 0$  and  $\bar{f}_e$  maximizes  $f_e$  over any  $u_e$  and  $\rho_e \in (0, \bar{\rho}_e)$ . On the other hand, the function  $\bar{s}_e$  is highly dependent on the physical structure of the segment  $e$  as well as random events, such as accidents and temporary lane closures (see, e.g., [49], [52]).

<sup>3</sup>The parameter  $\tau_e \bar{u}_e$  is known as the backward wave speed (see, e.g., [53]).

The constraint above ensures that the highway is not congested regardless of the flow rates. Using the constraint above and the fundamental diagram approximation in (1), we obtain

$$f_e(t) = u_e(t)\rho_e(t), \quad \forall e \in \mathcal{E}, t \in \mathcal{T}. \quad (3)$$

Finally, based on the physical principle of conservation of mass, the discretized LWR model provides a set of difference equations for each road segment  $e$  which enable us to analyze the dynamics of traffic flows on highways [51], [55]. For each segment  $e = (v, v + 1) \in \mathcal{E}$ , the dynamics of  $\rho_e$  are determined by the *demand* flow  $f_e^D(t)$  from  $v$  and the *supply* flow  $f_e^S(t)$  to  $v + 1$  as follows:

$$\rho_e(t + 1) = \rho_e(t) + h_e(f_e^D(t) - f_e^S(t)), \quad \forall t \in \mathcal{T},$$

where  $h_e := \delta / \text{len}_e$ . For numerical stability,  $\delta$  must be selected such that  $h_e \leq 1 / \max_{t \in \mathcal{T}} \{u_e(t)\}$ ,  $\forall e \in \mathcal{E}$  [34].

The supply flow  $f_e^S(t)$  denotes the maximal flow that can be transferred through edge  $e$ , and is given by

$$f_e^S(t) = \begin{cases} u_e(t)\rho_e(t), & \text{if } \rho_e(t) \leq \rho_e^c(u_e(t)), \\ u_e(t)\rho_e^c(u_e(t)), & \text{otherwise,} \end{cases}$$

Notice that  $f_e^S(t) = f_e(t)$  when the highway segment  $e$  is not congested, i.e., the constraint in (2) is satisfied. Consider junction  $v \in \mathcal{V}_D$ , i.e., the junction  $v$  is a departure node of the preceding edge of  $e$  or that of some edge  $s$ . Since  $v \in \mathcal{V}_D$ , a fraction of the supply  $f_s^S(t)$  will depart the highway through an off-ramp edge  $s''$  and the rest will enter into succeeding segment  $e$ . Let  $r_s^o(t) \in [0, 1)$  denote the fraction of the supply  $f_s^S(t)$  that departs the system. Hence, the flow through the off-ramp edge  $s''$  is  $f_{s''}(t) := r_s^o(t)f_s^S(t)$ . Notice that the fraction  $r_s^o(t)$  is determined by the drivers' actions. Therefore,  $r_s^o$  is random, and its value is unknown to the system operator in advance. Each random variable  $r_s^o(t)$  will have a nonempty support set denoted by  $\mathcal{Z}_{r_s^o(t)} \subset \mathbb{R}_{\geq 0}$ .

The traffic demand  $f_e^D(t)$  depends on the supply of its preceding edge  $s \in \mathcal{E}$  as well as the ramp flows on their connected junction  $v$ . At each  $v \in \mathcal{V}_A$ , a fraction of the traffic demand  $f_e^D(t)$  is originated from the on-ramp edge  $e'$ . Let  $r_e^{\text{in}}(t) \in [0, 1)$  denote the fraction of the traffic demand  $f_e^D(t)$  originated from the on-ramp edge  $e'$ . Hence, the on-ramp traffic flow is given by  $f_{e'}(t) := r_e^{\text{in}}(t)f_e^D(t)$ . Notice that the ratio  $r_e^{\text{in}}(t)$  is an exogenous parameter that depends on the traffic flow at the on-ramp edge  $e'$ . Hence, each ratio  $r_e^{\text{in}}(t)$  can be modeled as a random variable with nonempty support  $\mathcal{Z}_{r_e^{\text{in}}(t)} \subset \mathbb{R}_{\geq 0}$ <sup>4</sup>. Then, by the conservation of flows, at each time slot  $t$ , the traffic demand  $f_e^D(t)$  must satisfy the following constraint:

$$f_e^D(t) = f_s^S(t) - f_{s''}(t) + f_{e'}(t), \quad \forall t \in \mathcal{T}.$$

At edge  $e = (0, 1)$ , we have  $f_e^D(t) := \omega(t)$  which is a random mainstream with support  $\mathcal{Z}_{\omega(t)} \subset \mathbb{R}_{\geq 0}$ . At each edge  $e$ , the demand  $f_e^D(t)$  must be admissible to edge  $e$ , i.e.,

$$f_e^D(t) \leq \min\{\bar{f}_e, \tau_e \bar{u}_e (\bar{\rho}_e - \rho_e(t))\}. \quad (4)$$

Notice that, the constraints (4) allows for transient speed of  $f_e^D(t)$  higher than speed limit  $u_e(t)$ , as long as the mean speed  $s_e(t)$  complies with  $u_e(t)$ .

<sup>4</sup>For  $v \notin \mathcal{V}_D$  or  $v \notin \mathcal{V}_A$ , the value of  $r_s^o(t)$  or  $r_e^{\text{in}}(t)$  is zero, respectively.

Let  $\rho(0) = (\rho_1(0), \dots, \rho_n(0))$  denote the traffic density of the highway with support  $\mathcal{Z}_{\rho(0)} \subset \mathbb{R}_{\geq 0}^n$ . Using the constraints above, the traffic density dynamics at each time slot  $t \in \mathcal{T}$  are given by

$$\begin{aligned} \rho_e(t+1) &= \rho_e(t) + h_e \frac{1 - r_s^o(t)}{1 - r_e^{\text{in}}(t)} f_s(t) - h_e f_e(t), \\ &\quad \forall e \in \mathcal{E} \setminus \{(0, 1)\}, \\ \rho_e(t+1) &= \rho_e(t) + h_e(\omega(t) - f_e(t)), \quad e = (0, 1). \end{aligned} \quad (5)$$

Recall that  $f_e(t) = u_e(t)\rho_e(t)$ . For each  $e \in \mathcal{E} \setminus \{(0, 1)\}$  and  $t \in \mathcal{T}$ , the constraint in (4) can be written as

$$\frac{1 - r_s^o(t)}{1 - r_e^{\text{in}}(t)} f_s(t) \leq \min\{\bar{f}_e, \tau_e \bar{u}_e (\bar{\rho}_e - \rho_e(t))\}, \quad (6)$$

where  $s$  is the preceding edge of edge  $e$ .

Our goal is to design a set of speed limits for drivers. To achieve this goal, we consider a finite set of speed limits, and then approximate the fundamental diagram of each segment  $e$  with a finite set of piece-wise linear functions, as shown in Fig. 2. Let  $\Gamma$  be a finite set of feasible speed limits for the highway segments. More precisely, the speed limit of each edge  $e \in \mathcal{E}$  must satisfy

$$u_e(t) \in \Gamma := \{\gamma^{(1)}, \dots, \gamma^{(m)}\}, \quad t \in \mathcal{T}. \quad (7)$$

The set of real values  $\Gamma$  is determined by the physical structure of the highway as well as its maximal free flow speed and traffic jam density. As mentioned earlier, random events, such as traffic incidents or lane closure, can change these values.

### C. Problem Formulation for the Traffic Control Problem

We aim at maximizing the expected flow rate of highway segments while reducing congestion via speed limits. To compute the average flow, let  $\mathbb{P}_{\varpi}$  denote the distribution of the concatenated random variable  $\varpi := (\omega, \rho(0), r^{\text{in}}, r^o)$ . Given the parameters  $\{\bar{f}_e\}_{e \in \mathcal{E}}$ ,  $\{\bar{\rho}_e\}_{e \in \mathcal{E}}$ , and  $\Gamma$ , the problem of computing speed limits which maximize the expected flow, can be formulated as follows:

$$\begin{aligned} (\mathbf{P}) \quad & \max_{u, \rho} \quad \mathbb{E}_{\mathbb{P}_{\varpi}} \left[ \frac{1}{T} \sum_{e \in \mathcal{E}, t \in \mathcal{T}} \rho_e(t) u_e(t) \right], \\ & \text{s. t.} \quad (2), (3), (5), (6), (7), \end{aligned}$$

where  $\rho$  and  $u$  are the concatenated variables of  $\{\rho_e(t)\}_{e \in \mathcal{E}, t \in \mathcal{T}}$ <sup>5</sup> and  $\{u_e(t)\}_{e \in \mathcal{E}, t \in \mathcal{T}}$ , respectively.

Problem (P) is nonconvex. In addition, the probability distribution  $\mathbb{P}_{\varpi}$  is unknown, i.e., it is impossible to compute the expected flow (i.e., the objective function) exactly. Our goal is to compute a set of speed limits that are feasible to Problem (P) and guarantee a minimum achievable expected flow in the presence of uncertainty on  $\mathbb{P}_{\varpi}$ . To achieve this goal, we adapt the proposed framework to compute the desired speed limits. In this way, given an optimal speed limit  $u$  and a set of  $N$  samples, we obtain  $J(u)$ , an achievable average flow rate—let us call it certificate. In particular,  $J(u)$  is a function of the  $N$  random samples. This certificate is a minimum with confidence  $\beta \in (0, 1)$  in the sense that the probability of the true objective function being greater than  $J(u)$  is greater than  $1 - \beta$ . In other words, let  $\text{Prob}^N$  denote the

<sup>5</sup> $\rho := (\rho_1(0), \rho_2(0), \dots, \rho_n(0), \rho_1(1), \dots, \rho_n(T-1))$ .



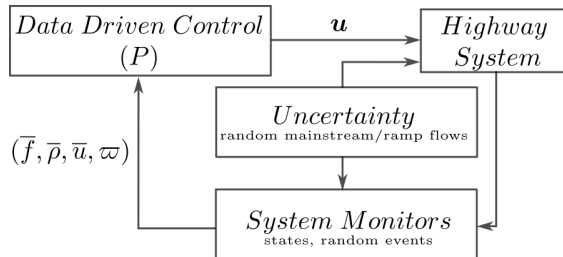


Fig. 3: Data-driven speed-limit control on highways under random ramp flows and system events.

product probability distribution over  $N$  samples. Under certain conditions on  $\mathbb{P}_\varpi$ , the proposed approach guarantees that the following out-of-sample performance constraint is satisfied:

$$\text{Prob}^N \left( \mathbb{E}_{\mathbb{P}_\varpi} \left[ \frac{1}{T} \sum_{e \in \mathcal{E}, t \in \mathcal{T}} \rho_e(t) u_e(t) \right] \geq J(u) \right) \geq 1 - \beta. \quad (8)$$

The probabilistic guarantee (8) enables us to evaluate the performance of a feasible solution  $u$  to Problem (P) via only finite samples of  $\varpi$  and a lower bound  $J(u)$ . We call a solution  $u$  with the probabilistic guarantee (8) a *data-driven Speed-Limit control*.

**Remark II.1 (Implementation of data-driven control)** With online-accessible samples of  $\varpi$  and parameters  $(\bar{f}, \bar{\rho}, \bar{u})$  which are related to real-time highway random events, the data-driven control  $u$  can be achieved via online solutions to (P) in a moving horizon fashion. Fig. 3 demonstrates how to implement the proposed approach in real-world applications.

**Remark II.2 (Admissible operation zone)** In this work, we propose a set of speed-limit controls that prevents congestion with probabilistic guarantees. Note that the existence of such controls is highly dependent on the feasibility of Problem (P). When traffic demands are higher than the highway capacity in a sufficiently long time, congestion is inevitable. Therefore, there is no hope to prevent congestion via the speed-limit control in the presence of high traffic demands. In such scenarios, we set speed limits to a set of predefined values.

### III. PERFORMANCE GUARANTEED SPEED-LIMIT DESIGN

Our goal is to compute a set of speed limits with certain out-of-sample performance guarantees. To achieve this goal, we follow a four-step procedure. First, we reformulate Problem (P) into an equivalent problem (call it Problem (P1)). Second, we propagate the admissible sample trajectories using the  $N$  measurements of  $\varpi$ . Third, we adopt a distributionally robust optimization approach to (P1). The first three steps enable us to obtain a distributionally robust optimization framework for computing speed limits with guarantees equivalent to (8). Finally, we obtain a tractable problem reformulation.

**Step 1: (Equivalent Reformulation of (P))** Traffic densities  $\rho_e(t)$ , for all  $e \in \mathcal{E}$  and  $t \in \mathcal{T}$ , are random since traffic inflows and outflows are random in each segment  $e$ . Using this observation, we now consider the variable  $\rho$  in Problem (P) as a random variable, and derive an equivalent Problem (P1) via a reformulation of the constraints in (P).

Given a speed limit  $u$  that satisfies the constraint (7), let  $\mathbb{P}(u)$  and  $\mathcal{Z}(u)$  denote the probability distribution of variable  $\rho$  and the support of  $\rho$ , respectively.<sup>6</sup> Recall that in Problem (P), constraints (2) ensure no congestion on the highway. Hence, the given  $u$  should be such that  $\mathcal{Z}(u) \subseteq \{\rho \in \mathbb{R}^{nT} \mid (2)\}$ . Without loss of generality, we consider the largest possible support  $\mathcal{Z}(u) := \{\rho \in \mathbb{R}^{nT} \mid (2)\}$ . To fully characterize random variable  $\rho$ , the distribution of  $\mathbb{P}(u)$  needs to be determined. Using the traffic density dynamics in (5), flow representation in (3) and sustainability constraints in (6), the probability distribution  $\mathbb{P}(u)$  can be represented as a convolution of the distribution  $\mathbb{P}_{\varpi}$ .

Let  $\mathcal{M}(\mathcal{Z}(u))$  denote the space of all probability distributions supported on  $\mathcal{Z}(u)$ . Let us write the objective function of Problem (P) compactly as

$$H(u; \rho) := \frac{1}{T} \sum_{e \in \mathcal{E}, t \in \mathcal{T}} \rho_e(t) u_e(t),$$

and reformulate (P) as follows

$$\begin{aligned} \text{(P1)} \quad & \max_u \quad \mathbb{E}_{\mathbb{P}(u)} [H(u; \rho)], \\ & \text{s. t.} \quad \mathbb{P}(u) \text{ characterized by (3), (5), (6) and } \mathbb{P}_{\varpi}, \\ & \quad \mathbb{P}(u) \in \mathcal{M}(\mathcal{Z}(u)), \text{ (7)}. \end{aligned}$$

Notice that Problems (P) and (P1) are equivalent. Hence, we obtain the performance guarantee of (P1) by considering the induced out-of-sample performance on  $\mathbb{P}(u)$ , written as  $\mathbb{E}_{\mathbb{P}(u)} [H(u; \rho)]$ . For all problems derived later, we use the performance guarantees equivalent to (8), as follows

$$\text{Prob}^N \left( \mathbb{E}_{\mathbb{P}(u)} [H(u; \rho)] \geq J(u) \geq 1 - \beta. \right) \quad (9)$$

Recall that  $\text{Prob}^N$  denotes the probability that the event  $\mathbb{E}_{\mathbb{P}(u)} [H(u; \rho)] \geq J(u)$  happens on the  $N$  product of the sample space that defines  $\rho$ , the value  $J(u)$  is the certificate to be determined, and  $\beta \in (0, 1)$  is the desired confidence value.

Next, we characterize the probability distribution  $\mathbb{P}(u)$  using the  $N$  sample measurements of  $\varpi$ .

**Step 2: (Admissible Sample Trajectory Propagation)** Let  $\mathcal{L} = \{1, \dots, N\}$  denote the index set for the  $N$  realizations of the random variable  $\varpi$ , and let  $\{\varpi^{(l)}\}_{l \in \mathcal{L}}$ , where  $\varpi^{(l)} := (\omega^{(l)}, \rho^{(l)}(0), r^{\text{in},(l)}, r^{\text{o},(l)})$ , denote the set of independent and identically distributed (i.i.d.) realizations of  $\varpi$ . Given a speed limit  $u$  and measurement  $\varpi^{(l)}$ , a unique traffic density trajectory  $\rho^{(l)}$  can be computed by using (3), (5). Notice that this trajectory is unique since density dynamics (5) is linear (in  $\rho$ ) for a given speed limit  $u$  and measurement  $\varpi^{(l)}$ . Further, the resulting  $\rho^{(l)}$  is an *admissible* traffic trajectory if the given  $u$  achieves the flow sustainability constraints (6). Given these realizations  $\{\varpi^{(l)}\}_{l \in \mathcal{L}}$ , the admissible sample trajectories  $\{\rho^{(l)}\}_{l \in \mathcal{L}}$  of the random traffic flow densities for each edge  $e \in \mathcal{E}$  with its precedent  $s \in \mathcal{E} \cup \emptyset$ , are given by

$$\begin{aligned} \rho_e^{(l)}(t+1) &= h_e \frac{1 - r_s^{\text{o},(l)}(t)}{1 - r_e^{\text{in},(l)}(t)} u_s(t) \rho_s^{(l)}(t) - h_e u_e(t) \rho_e^{(l)}(t) \\ &\quad + \rho_e^{(l)}(t), \quad \forall e \in \mathcal{E} \setminus \{(0, 1)\}, \\ \rho_e^{(l)}(t+1) &= \rho_e^{(l)}(t) + h_e (\omega^{(l)}(t) - u_e(t) \rho_e^{(l)}(t)), \quad e = (0, 1), \\ \frac{1 - r_s^{\text{o},(l)}(t)}{1 - r_e^{\text{in},(l)}(t)} u_s(t) \rho_s^{(l)}(t) &\leq \min \left\{ \bar{f}_e, \tau_e \bar{u}_e \left( \bar{\rho}_e - \rho_e^{(l)}(t) \right) \right\}, \\ &\quad \forall e \in \mathcal{E} \setminus \{(0, 1)\}, \end{aligned} \quad (10)$$

<sup>6</sup>The support  $\mathcal{Z}(u)$  is the smallest closed set such that  $P(\rho \in \mathcal{Z}(u)) = 1$ .

for all  $t \in \mathcal{T}$  and  $l \in \mathcal{L}$ . The following lemma establishes that  $\{\rho^{(l)}\}_{l \in \mathcal{L}}$  are i.i.d. samples from  $\mathbb{P}(u)$ .

**Lemma III.1 (Independent and identically distributed sample generators of  $\rho$ )** *Given a speed limit  $u$  and a set of i.i.d. realizations of  $\varpi$ , the system dynamics (10) generate i.i.d. admissible sample trajectories  $\{\rho^{(l)}\}_{l \in \mathcal{L}}$  of  $\mathbb{P}(u)$ .*

The proof is provided in Appendix A, which also contains all the proofs of the later lemmas, propositions and theorems.

Let  $\mathcal{M}_{\text{lt}}(\mathcal{Z}_\varpi) \subset \mathcal{M}(\mathcal{Z}_\varpi)$  denote the space of all light-tailed probability distributions supported on  $\mathcal{Z}_\varpi$ <sup>7</sup>. We make the following assumption on the probability distribution  $\mathbb{P}_\varpi$ :

**Assumption III.1 (Light-tailed unknown distributions)** *The distribution  $\mathbb{P}_\varpi$  satisfies  $\mathbb{P}_\varpi \in \mathcal{M}_{\text{lt}}(\mathcal{Z}_\varpi)$ , i.e., there exists an exponent  $a > 1$  such that  $b := \mathbb{E}_{\mathbb{P}_\varpi} [\exp(\|\varpi\|^a)] < \infty$ .*

**Remark III.1 (Accessible light-tailed i.i.d. samples of  $\varpi$ )** The random variable  $\varpi$  essentially represents the random flows and densities on the highway. This results into an unknown compact support of  $\mathbb{P}_\varpi$ , indicating that  $\mathbb{P}_\varpi$  is also light-tailed. Further, online samples of  $\varpi$  can come from various independent system monitors, e.g., Traffic Performance Measurement Systems (T-PeMS), or real-time GPS systems, which provide online i.i.d. samples of  $\varpi$ .

The following lemma establishes that the probability distribution of traffic densities is light-tailed when  $\mathbb{P}_\varpi$  is light-tailed.

**Lemma III.2 (Light-tailed distribution of  $\rho$ )** *Let Assumption III.1 hold, then  $\mathbb{P}(u) \in \mathcal{M}_{\text{lt}}(\mathcal{Z}(u))$ .*

The above Lemmas III.1 and III.2 enable the application of the proposed framework to (P1) in the next step.

**Step 3: (Performance Guarantee Certificate)** Given a speed limit  $u$ , we design a certificate  $J(u)$  that satisfies the performance guarantee condition (9). To achieve this goal, the proposed approach consists of solving a robust version of the problem over a set of distributions. In particular, we will consider a set of distributions  $\mathcal{P}(u)$  that is small, tractable and yet rich enough to contain  $\mathbb{P}(u)$  with high probability. Then by evaluating (P1) under the worst-case distribution in  $\mathcal{P}(u)$ , the performance of (P1) in the form of (9) can be guaranteed.

Consider the Wasserstein ball<sup>8</sup>  $\mathbb{B}_\epsilon(\hat{\mathbb{P}}(u))$  of center  $\hat{\mathbb{P}}(u) := (1/N) \sum_{l \in \mathcal{L}} \delta_{\{\rho^{(l)}\}}$  and radius  $\epsilon$ . Notice that the center  $\hat{\mathbb{P}}(u)$  is obtained using the point mass operator  $\delta$  under i.i.d. admissible sample trajectories  $\{\rho^{(l)}\}_{l \in \mathcal{L}}$ . These trajectories are distributed according to  $\mathbb{P}(u)$  which is a function of the controlled system dynamics (10) and samples of  $\varpi$ . Then we propose certificates  $J(u)$  of (P1) in the following theorem.

<sup>7</sup>For any set  $\mathcal{Z}$ , we use notion  $\mathcal{M}_{\text{lt}}(\mathcal{Z})$  to denote the space of all light-tailed probability distributions supported on  $\mathcal{Z}$ .

<sup>8</sup>Let  $\mathcal{M}(\mathcal{Z})$  denote the space of all probability distributions supported on  $\mathcal{Z}$ . Then for any two distributions  $\mathbb{Q}_1, \mathbb{Q}_2 \in \mathcal{M}(\mathcal{Z})$ , the Wasserstein metric [56]  $d_W : \mathcal{M}(\mathcal{Z}) \times \mathcal{M}(\mathcal{Z}) \rightarrow \mathbb{R}_{\geq 0}$  is defined by

$$d_W(\mathbb{Q}_1, \mathbb{Q}_2) := \min_{\Pi} \int_{\mathcal{Z} \times \mathcal{Z}} \|\xi_1 - \xi_2\| \Pi(d\xi_1, d\xi_2),$$

where  $\Pi$  is in a set of all distributions on  $\mathcal{Z} \times \mathcal{Z}$  with marginals  $\mathbb{Q}_1$  and  $\mathbb{Q}_2$ . A closed Wasserstein ball of radius  $\epsilon$  centered at a distribution  $\mathbb{P} \in \mathcal{M}(\mathcal{Z})$  is denoted by  $\mathbb{B}_\epsilon(\mathbb{P}) := \{\mathbb{Q} \in \mathcal{M}(\mathcal{Z}) \mid d_W(\mathbb{P}, \mathbb{Q}) \leq \epsilon\}$ .

**Theorem III.1 (Performance guarantees of (P1))** *Let us assume that  $N$  i.i.d. samples of  $\varpi$  are given, together with a speed limit  $u$ , and confidence value  $\beta$ , and that Assumption III.1 on light-tailed distributions of  $\varpi$  holds. Further, let us define the set of distributions  $\mathcal{P}(u)$  as follows:*

$$\mathcal{P}(u) := \mathbb{B}_{\epsilon(\beta)}(\hat{\mathbb{P}}(u)) \cap \mathcal{M}_{\text{lt}}(\mathcal{Z}(u)).$$

*Then, there exists a Wasserstein radius  $\epsilon := \epsilon(\beta)$ , depending on the confidence value  $\beta$  and Assumption III.1, such that  $\mathbb{P}(u)$  is in the set of distributions  $\mathcal{P}(u)$  as described in (P1) with probability at least  $1 - \beta$ , i.e.,*

$$\text{Prob}^N (\mathbb{P}(u) \in \mathcal{P}(u)) \geq 1 - \beta.$$

*Further, the following proposed certificate  $J(u)$  of (P1) satisfies guarantee (9)*

$$J(u) := \inf_{\mathbb{Q} \in \mathcal{P}(u)} \mathbb{E}_{\mathbb{Q}} [H(u; \rho)].$$

**Remark III.2 (Effect of Assumption III.1 on  $J(u)$ )** The certificate  $J(u)$  highly depends on the set  $\mathcal{P}(u)$  and the Wasserstein radius  $\epsilon(\beta)$ . In Theorem III.1, the value  $\epsilon(\beta)$  is calculated via the parameters  $a$  and  $b$  in Assumption III.1. As these parameters may not be known, one can determine  $\epsilon(\beta)$  in a data driven fashion via Monte-Carlo simulations. That is, we start by setting  $\epsilon(\beta) = 0$  and gradually increase it until the performance guarantees (9) hold with that given  $\beta$  for a sufficiently large number of simulation runs.

Theorem III.1 provides each feasible solution  $u$  of (P1) with a certificate  $J(u)$  that guarantees performance as in (9). This motivates a tractable reformulation of (P1) as follows.

**Step 4: (Tractable Reformulation of (P1))** Our goal is to obtain a speed limit  $u$  that maximizes the average flow through the highway as in (P1) while ensuring that the performance guarantee condition (9) is satisfied. Given a set of inflow-and-outflow-related samples  $\{\varpi^{(l)}\}_{l \in \mathcal{L}}$ , a speed limit  $u$  that provides the highest  $J(u)$  (i.e., the best objective lower bound), can be computed by solving the following optimization problem:

$$\text{(P2)} \quad \sup_{u \text{ s.t. (7)}} J(u).$$

Problem (P2) is an infinite-dimensional optimization problem, and, hence, it is hard to solve. The following theorem, provides a finite-dimensional reformulation of Problem (P2), called (P3), and shows that problems (P2) and (P3) are equivalent for  $(u, J)$ .

**Theorem III.2 (Tractable reformulation of (P2))** *Consider*

$$\begin{aligned} \text{(P3)} \quad & \max_{u, \rho, \lambda, \mu, \nu, \eta} \quad -\lambda \epsilon(\beta) - \frac{1}{N} \sum_{e \in \mathcal{E}, t \in \mathcal{T}, l \in \mathcal{L}} \bar{f}_e \bar{\rho}_e \eta_e^{(l)}(t) \\ & \quad + \frac{1}{N} \sum_{l \in \mathcal{L}} \langle \nu^{(l)}, \rho^{(l)} \rangle, \\ \text{s. t.} \quad & [\bar{f} \otimes \mathbf{1}_T + (\bar{\rho} - \rho^c(\bar{u})) \otimes \mathbf{1}_T \circ u] \circ \eta^{(l)} \\ & \quad - \mu^{(l)} \geq \mathbf{0}_{nT}, \quad \forall l \in \mathcal{L}, \\ & \nu^{(l)} = \mu^{(l)} + \frac{1}{T} u, \quad \forall l \in \mathcal{L}, \\ & \|\nu^{(l)}\|_* \leq \lambda, \quad \forall l \in \mathcal{L}, \end{aligned}$$

$$\eta^{(l)} \geq \mathbf{0}_{nT}, \forall l \in \mathcal{L},$$

(7), (10),

where decision variables  $(u, \rho, \lambda, \mu, \nu, \eta)$  are concatenated versions of  $u_e(t)$ ,  $\rho_e^{(l)}(t)$ ,  $\lambda$ ,  $\mu_e^{(l)}(t)$ ,  $\nu_e^{(l)}(t)$ ,  $\eta_e^{(l)}(t) \in \mathbb{R}$ , for all  $l \in \mathcal{L}$ ,  $t \in \mathcal{T}$ , and  $e \in \mathcal{E}$ . The value  $\rho^c(\bar{u}) := \bar{f}/\bar{u}$  is the vector of critical densities under the free flow, and  $\bar{\rho}$  is the jam density vector.

Problem (P2) is equivalent to (P3) in the sense that their optimal objective values coincide and the set of optimizers of (P2) are the projection of that of (P3). Further, for any feasible point  $(u, \rho, \lambda, \mu, \nu, \eta)$  of (P3), let  $\hat{J}(u)$  denote the value of its objective function. Then the pair  $(u, \hat{J}(u))$  gives a data-driven solution  $u$  with an estimate of its certificate  $J(u)$  by  $\hat{J}(u)$ , such that the performance guarantee (9) holds for  $(u, \hat{J}(u))$ .

**Remark III.3 (Formulation (P3) depends on data)** Problem (P3) is parameterized by the variables  $(\bar{f}, \bar{\rho}, \bar{u})$ , which are related to the highway infrastructure and random events, and the data  $\{\varpi^{(l)}\}_{l \in \mathcal{L}}$ , which are related to the traffic system initial state,  $\{\rho^{(l)}(0)\}_{l \in \mathcal{L}}$ , on-ramp, and off-ramp flows. The decision variables include future states of the density  $\rho^{(l)}(t)$ ,  $t > 0$ , the speed limits, and other multipliers to make the constraints hold. In particular, note that the ambiguity-ball constraint is enforced via the  $\lambda$  multiplier and maximization in  $\rho$ . In practice, highway random events such as accidents are monitored in real time, which provides particular information about  $(\bar{f}, \bar{\rho}, \bar{u})$ . On the other hand, data  $\{\varpi^{(l)}\}_{l \in \mathcal{L}}$  is accessible from various independent monitors as mentioned in the previous remark on data-driven control implementation.

Problem (P3) is inherently difficult to solve due to the discrete decision variables  $u$ , bi-linear terms  $u \circ \eta^{(l)}$  in the first group of constraints, and the nonlinear admissible sample trajectories  $\{\rho^{(l)}\}_{l \in \mathcal{L}}$ , which motivates our next section.

#### IV. EQUIVALENT REFORMULATION

Our goal is to compute exact solutions to Problem (P3). To achieve this goal, we focus on the feasibility set of Problem (P3), and transform a group of its non-convex quadratic terms, which are comprised of a continuous variable and a binary variable, into a set of mixed-integer linear constraints. We call the new equivalent formulation, Problem (P4).

**Binary Representation of Speed Limits:** Let  $\mathcal{O} := \{1, \dots, m\}$  be the index set of the speed limit set  $\Gamma$ . For each edge  $e \in \mathcal{E}$ , time slot  $t \in \mathcal{T}$  and speed limit value  $\gamma^{(i)} \in \Gamma$ , let us define the binary variable  $x_{e,i}(t)$  to be equal to one if  $u_e(t) = \gamma^{(i)}$ ; otherwise  $x_{e,i}(t) = 0$ . We will then have  $u_e(t) = \sum_{i \in \mathcal{O}} \gamma^{(i)} x_{e,i}(t)$  for each edge  $e \in \mathcal{E}$ . Using this representation, we can reformulate the speed limit constraints (7) as follows

$$\begin{aligned} \gamma^{(1)} &\leq \sum_{i \in \mathcal{O}} \gamma^{(i)} x_{e,i}(t) \leq \gamma^{(m)}, \forall e \in \mathcal{E}, \forall t \in \mathcal{T}, \\ \sum_{i \in \mathcal{O}} x_{e,i}(t) &= 1, \forall e \in \mathcal{E}, \forall t \in \mathcal{T}, \\ x_{e,i}(t) &\in \{0, 1\}, \forall e \in \mathcal{E}, i \in \mathcal{O}, t \in \mathcal{T}, \end{aligned} \tag{11}$$

and we update the admissible sample trajectories formula (10) for all  $t \in \mathcal{T}$  and  $l \in \mathcal{L}$  as follows

$$\begin{aligned}\rho_e^{(l)}(t+1) &= h_e \frac{1 - r_s^{o,(l)}(t)}{1 - r_e^{in,(l)}(t)} \sum_{i \in \mathcal{O}} \gamma^{(i)} x_{s,i}(t) \rho_s^{(l)}(t) + \rho_e^{(l)}(t) \\ &\quad - h_e \sum_{i \in \mathcal{O}} \gamma^{(i)} x_{e,i}(t) \rho_e^{(l)}(t), \quad \forall e \in \mathcal{E} \setminus \{(0,1)\}, \\ \rho_e^{(l)}(t+1) &= \rho_e^{(l)}(t) + h_e \omega^{(l)}(t) - h_e \sum_{i \in \mathcal{O}} \gamma^{(i)} x_{e,i}(t) \rho_e^{(l)}(t), \\ &\quad e = (0,1).\end{aligned}\tag{12}$$

$$\begin{aligned}\frac{1 - r_s^{o,(l)}(t)}{1 - r_e^{in,(l)}(t)} \sum_{i \in \mathcal{O}} \gamma^{(i)} x_{s,i}(t) \rho_s^{(l)}(t) &\leq \\ \min \left\{ \bar{f}_e, \tau_e \bar{u}_e \left( \bar{\rho}_e - \rho_e^{(l)}(t) \right) \right\}, &\quad \forall e \in \mathcal{E} \setminus \{(0,1)\},\end{aligned}$$

We are particularly interested in two groups of bi-linear terms: 1) the bi-linear terms  $x_{e,i}(t) \rho_e^{(l)}(t)$  in the admissible sample trajectories formula (12) and 2) the bi-linear terms  $\sum_{i \in \mathcal{O}} \gamma^{(i)} x_{e,i}(t) \eta_e^{(l)}(t)$  which appear in the first set of constraints, e.g.,  $u \circ \eta^{(l)}$ . Each of these bi-linear terms is comprised of a continuous variable and a binary variable. We represent each of these bi-linear terms with a set of linear constraints using the following linearization technique.

Let us introduce variables  $y_{e,i}^{(l)}(t)$  and  $z_{e,i}^{(l)}(t)$  for all  $e \in \mathcal{E}$ ,  $i \in \mathcal{O}$ ,  $t \in \mathcal{T}$  and  $l \in \mathcal{L}$  as follows

$$\begin{aligned}y_{e,i}^{(l)}(t) &= x_{e,i}(t) \rho_e^{(l)}(t), \\ z_{e,i}^{(l)}(t) &= x_{e,i}(t) \eta_e^{(l)}(t).\end{aligned}\tag{13}$$

We further make the following assumption

**Assumption IV.1 (Bounded dual variable  $\eta$ )** *There exists a positive constant  $\bar{\eta}$  such that for any optimizers of (P3), the components  $\eta_e^{(l)}(t) \leq \bar{\eta}$  for all  $e \in \mathcal{E}$ ,  $t \in \mathcal{T}$  and  $l \in \mathcal{L}$ .*

We achieve Assumption IV.1 by selecting  $\bar{\eta}$  large enough. This enables the following lemma to represent the non-convex equality constraint in (13) with a set of linear constraints.

**Lemma IV.1 (Linearization technique)** *Let Assumption IV.1 hold. Then for all  $e \in \mathcal{E}$ ,  $i \in \mathcal{O}$ ,  $t \in \mathcal{T}$  and  $l \in \mathcal{L}$ , the non-convex equality constraint in (13) can be equivalently represented with the following set of linear constraints*

$$\begin{aligned}0 \leq z_{e,i}^{(l)}(t) &\leq \bar{\eta} x_{e,i}(t), \\ \eta_e^{(l)}(t) - \bar{\eta}(1 - x_{e,i}(t)) &\leq z_{e,i}^{(l)}(t) \leq \eta_e^{(l)}(t),\end{aligned}\tag{14}$$

$$\begin{aligned}0 \leq y_{e,i}^{(l)}(t) &\leq \bar{\rho}_e x_{e,i}(t), \\ \rho_e^{(l)}(t) - \bar{\rho}_e(1 - x_{e,i}(t)) &\leq y_{e,i}^{(l)}(t) \leq \rho_e^{(l)}(t).\end{aligned}\tag{15}$$

In particular, we let  $y_{e,i}^{(l)}(0) = x_{e,i}(0) \rho_e^{(l)}(0)$  for each  $e \in \mathcal{E}$ ,  $i \in \mathcal{O}$  and  $l \in \mathcal{L}$ . Then using the new variables  $y_{e,i}^{(l)}(t)$  and  $z_{e,i}^{(l)}(t)$ , we can now reformulate the admissible sample trajectories formula (12) as follows

$$\begin{aligned}
\rho_e^{(l)}(t+1) &= h_e \frac{1 - r_s^{o,(l)}(t)}{1 - r_e^{in,(l)}(t)} \sum_{i \in \mathcal{O}} \gamma^{(i)} y_{s,i}^{(l)}(t) + \rho_e^{(l)}(t) \\
&\quad - h_e \sum_{i \in \mathcal{O}} \gamma^{(i)} y_{e,i}^{(l)}(t), \quad \forall e \in \mathcal{E} \setminus \{(0,1)\}, \\
\rho_e^{(l)}(t+1) &= \rho_e^{(l)}(t) + h_e \omega^{(l)}(t) - h_e \sum_{i \in \mathcal{O}} \gamma^{(i)} y_{e,i}^{(l)}(t), \\
&\quad e = (0,1).
\end{aligned} \tag{16}$$

$$\begin{aligned}
&\frac{1 - r_s^{o,(l)}(t)}{1 - r_e^{in,(l)}(t)} \sum_{i \in \mathcal{O}} \gamma^{(i)} y_{s,i}^{(l)}(t) \leq \\
&\min \left\{ \bar{f}_e, \tau_e \bar{u}_e \left( \bar{\rho}_e - \rho_e^{(l)}(t) \right) \right\}, \quad \forall e \in \mathcal{E} \setminus \{(0,1)\},
\end{aligned}$$

Problem **(P3)** can now be equivalently reformulated as the following optimization problem

$$\begin{aligned}
\text{(P4)} \quad &\max_{\substack{x,y,z,\rho, \\ \lambda,\mu,\nu,\eta}} -\lambda \epsilon(\beta) - \frac{1}{N} \sum_{e,t,l} \bar{f}_e \bar{\rho}_e \eta_e^{(l)}(t) + \frac{1}{N} \sum_{e,t,l} \nu_e^{(l)}(t) \rho_e^{(l)}(t), \\
\text{s. t.} \quad &\sum_{i \in \mathcal{O}} \gamma^{(i)} (\bar{\rho} - \rho^c(\bar{u})) \otimes \mathbf{1}_T \circ z_i^{(l)} - \mu^{(l)} \\
&\quad + \bar{f} \otimes \mathbf{1}_T \circ \eta^{(l)} \geq \mathbf{0}_{nT}, \quad \forall l \in \mathcal{L}, \tag{17} \\
&\nu^{(l)} = \mu^{(l)} + \frac{1}{T} \sum_{i \in \mathcal{O}} \gamma^{(i)} x_i, \quad \forall l \in \mathcal{L}, \tag{18} \\
&\|\nu^{(l)}\|_* \leq \lambda, \quad \forall l \in \mathcal{L}, \tag{19} \\
&\mathbf{0}_{nT} \leq \eta^{(l)} \leq \bar{\eta}, \quad \forall l \in \mathcal{L}, \tag{20} \\
&\text{speed limits (11), dual variable (14),} \\
&\text{sample trajectories \{(15), (16)\}.}
\end{aligned}$$

**Remark IV.1 (Performance guarantee (9) in the setting of Problem (P4))** Let  $\hat{J}(u)$  denote the value of the objective function of **(P4)** at a computed feasible solution  $(x, y, z, \rho, \lambda, \mu, \nu, \eta)$ . Then, the resulting speed limits  $u := \sum_{i \in \mathcal{O}} \gamma^{(i)} x_i$  provide a data-driven solution such that  $(u, \hat{J}(u))$  satisfies the performance guarantee (9) of **(P1)**. This result exploits the fact that Problem **(P4)** is equivalent to **(P3)** and **(P3)** is equivalent to **(P2)** as in Theorem III.2.

## V. COMPUTATIONALLY EFFICIENT ALGORITHMS

We propose a decomposition-based, integer-solution search algorithm which computes online-tractable, high-quality feasible solutions to **(P4)** with performance guarantees. Similar algorithms have been proposed in the literature [57], [58]. Such methods allow us to compute sub-optimal solutions to mix-integer nonlinear programs efficiently. The proposed integer-solution search algorithm is shown in Algorithm 2. This algorithm iteratively computes sub-optimal solutions to **(P4)** until a stopping criteria is met. At each iteration, the algorithm solves an upper-bounding problem to **(P4)**, and then solves a lower-bounding problem to **(P4)**. The upper-bounding Problem (**UBP<sub>k</sub>**) is obtained through McCormick relaxations of the bi-linear terms  $\{\nu^{(l)} \circ \rho^{(l)}\}_{l \in \mathcal{L}}$ .

This upper bounding problem is a mixed-integer linear program and its solution provides us with an upper bound on Problem (P4) and a candidate speed limits  $x^{(k)}$ . Notice that  $x^{(k)}$  respects the sustainability constraints in (16). We then use the computed speed limit  $x^{(k)}$  to construct a set of admissible sample trajectories  $\{\rho^{(l,k)}\}_{l \in \mathcal{L}}$  and equivalently reduce Problem (P4) to a linear lower-bounding Problem (LBP<sub>k</sub>) for potential feasible solutions of (P4). If (LBP<sub>k</sub>) is feasible, then the candidate speed limits together with the objective value of (LBP<sub>k</sub>) provide guarantee (9) for (P4). Next, we present the upper-bounding and lower-bounding problems in detail.

---

**Algorithm 2** Integer solution search algorithm

---

- 1: Initialize  $k = 0$
  - 2: **repeat**
  - 3:      $k \leftarrow k + 1$
  - 4:     Solve Problem (UBP<sub>k</sub>), **return**  $x^{(k)}$  and  $\text{UB}_k$
  - 5:     Generate admissible sample trajectories  $\{\rho^{(l,k)}\}_{l \in \mathcal{L}}$
  - 6:     Solve Problem (LBP<sub>k</sub>), **return**  $\text{obj}_k$  and  $\text{LB}_k$
  - 7: **until**  $\text{UB}_k - \text{LB}_k \leq \epsilon$ , or (UBP<sub>k</sub>) is infeasible, or a satisfactory sub-optimal solution is found after certain running time  $T_{\text{run}}$
  - 8: **return** data driven solution  $u_{\text{best}} := u^{(q)}$  with certificate  $\hat{J}(u^{(q)})$  such that  $q \in \text{argmax}_{p=1, \dots, k} \{\text{obj}_p\}$
- 

### A. Upper-bounding Problem

Problem (UBP<sub>k</sub>) is constructed in two stages:

**Stage 1:** We use a standard McCormick relaxation to handle the non-convex quadratic terms  $\{\nu_e^{(l)}(t)\rho_e^{(l)}(t)\}_{e \in \mathcal{E}, t \in \mathcal{T}, l \in \mathcal{L}}$  in the objective function of (P4). Notice that the McCormick envelope [59] provides relaxations of bi-linear terms, which is stated in the following remark.

**Remark V.1 (McCormick envelope)** Consider two variables  $x, y \in \mathbb{R}$  with upper and lower bounds,  $\underline{x} \leq x \leq \bar{x}$ ,  $\underline{y} \leq y \leq \bar{y}$ . The McCormick envelope of the variable  $s := xy \in \mathbb{R}$  is characterized by the following constraints

$$\begin{aligned} s &\geq \bar{x}y + x\bar{y} - \bar{x}\bar{y}, & s &\geq \underline{x}y + x\underline{y} - \underline{x}\underline{y}, \\ s &\leq \bar{x}y + x\underline{y} - \bar{x}\underline{y}, & s &\leq \underline{x}y + x\bar{y} - \underline{x}\bar{y}. \end{aligned}$$

To construct a McCormick envelope for (UBP<sub>k</sub>), let us denote  $\bar{\nu}_e := \bar{u}_e(T^{-1} + \bar{\rho}_e\bar{\eta})$  for each edge  $e \in \mathcal{E}$ . We have  $0 \leq \nu_e^{(l)}(t) \leq \bar{\nu}_e$ ,  $0 \leq \rho_e^{(l)}(t) \leq \bar{\rho}_e$  for all  $e \in \mathcal{E}$ ,  $t \in \mathcal{T}$ , and  $l \in \mathcal{L}$ . Therefore, the McCormick envelope of  $s_e^{(l)}(t) := \nu_e^{(l)}(t)\rho_e^{(l)}(t)$  is given by

$$\begin{aligned} s_e^{(l)}(t) &\geq \bar{\nu}_e\rho_e^{(l)}(t) + \nu_e^{(l)}(t)\bar{\rho}_e - \bar{\nu}_e\bar{\rho}_e, \\ s_e^{(l)}(t) &\geq 0, \\ s_e^{(l)}(t) &\leq \bar{\nu}_e\rho_e^{(l)}(t), \\ s_e^{(l)}(t) &\leq \nu_e^{(l)}(t)\bar{\rho}_e. \end{aligned} \tag{21}$$

**Stage 2:** We identify appropriate canonical integer cuts to prevent (UBP<sub>k</sub>) from choosing examined candidate variable speed limits  $\{x^{(p)}\}_{p=1}^{k-1}$ . Let  $\Omega^{(p)} := \{(e, i, t) \in \mathcal{E} \times \mathcal{O} \times \mathcal{T} \mid x_{e,i}^{(p)}(t) = 1\}$



denote the index set of  $x$  for which the value  $x_{e,i}^{(p)}(t)$  is 1 at the previous iteration  $p$ . In addition, let  $c^{(p)} := |\Omega^{(p)}|$  and  $\bar{\Omega}^{(p)} := (\mathcal{E} \times \mathcal{O} \times \mathcal{T}) \setminus \Omega^{(p)}$  denote the cardinality of the set  $\Omega^{(p)}$  and the complement of  $\Omega^{(p)}$ , respectively. Therefore, the canonical integer cuts of Problem **(UBP<sub>k</sub>)** at iteration  $k$  are given by

$$\sum_{(e,i,t) \in \Omega^{(p)}} x_{e,i}(t) - \sum_{(e,i,t) \in \bar{\Omega}^{(p)}} x_{e,i}(t) \leq c^{(p)} - 1, \quad (22)$$

$$\forall p \in \{1, \dots, k-1\}.$$

Upper-bounding Problem **(UBP<sub>k</sub>)** can be formulated as follows

$$\begin{aligned} \text{(UBP}_k) \quad & \max_{\substack{x,y,z,s,\rho, \\ \lambda,\mu,\nu,\eta}} -\lambda\epsilon(\beta) - \frac{1}{N} \sum_{e,t,l} (\bar{f}_e \bar{\rho}_e \eta_e^{(l)}(t) - s_e^{(l)}(t)), \\ \text{s. t.} \quad & \text{speed limits (11), sample trajectories \{(15), (16)\},} \\ & \text{no congestion \{(14), (17), (18), (19), (20)\},} \\ & \text{McCormick envelope (21), integer cuts (22).} \end{aligned}$$

Let  $\text{UB}_k$  denote the optimal objective value of **(UBP<sub>k</sub>)**, and let  $x^{(k)}$  denote the integer part of the optimizers of **(UBP<sub>k</sub>)**. Then  $\text{UB}_k$  is an upper bound of the original non-convex Problem **(P4)**. We use  $x^{(k)}$  as a candidate speed limit in the lower-bounding problem **LBP<sub>k</sub>**.

### B. Lower-bounding Problem

Problem **(P4)** can be equivalently written as

$$\begin{aligned} & \max_{\substack{x,y,z,\rho, \\ \lambda,\mu,\nu,\eta}} -\lambda\epsilon(\beta) - \frac{1}{N} \sum_{e,t,l} (\bar{f}_e \bar{\rho}_e \eta_e^{(l)}(t) - \nu_e^{(l)}(t) \rho_e^{(l)}(t)), \\ \text{s. t.} \quad & (z, \lambda, \mu, \nu, \eta) \in \Phi(x), (y, \rho) \in \Psi(x), x \in X. \end{aligned}$$

where

$$\begin{aligned} \Phi(x) &:= \{(z, \lambda, \mu, \nu, \eta) \mid \text{no congestion}\}, \\ \Psi(x) &:= \{(y, \rho) \mid \text{sample trajectories}\}, \\ X &:= \{x \mid \text{speed limits}\}. \end{aligned}$$

The solution  $x^{(k)}$  to **(UBP<sub>k</sub>)** at iteration  $k$  provides us with a candidate speed limit  $u^{(k)} := \sum_{i \in \mathcal{O}} \gamma^{(i)} x_i^{(k)}$  which respect the sustainability constraints. For each  $l \in \mathcal{L}$  with the given  $u^{(k)}$ , the admissible sample trajectory  $\rho^{(l)}$  is uniquely determined by  $(\omega^{(l)}, \rho^{(l)}(0), r^{\text{in},(l)}, r^{\text{out},(l)})$  using the uniqueness solution of the linear time-invariant systems. Therefore, the element  $(y, \rho) \in \Psi(x^{(k)})$  is unique. Using the constraints set  $\Psi(x^{(k)})$ , we then construct the unique admissible sample

trajectories  $\{\rho^{(l,k)}\}_{l \in \mathcal{L}}$ . The unique admissible sample trajectories allow us to reduce **(P4)** to the following lower bounding problem<sup>9</sup>

$$\begin{aligned}
 (\text{LBP}_k) \quad & \max_{z, \lambda, \mu, \nu, \eta} -\lambda \epsilon(\beta) - \frac{1}{N} \sum_{e, t, l} (\bar{f}_e \bar{\rho}_e \eta_e^{(l)}(t) - \nu_e^{(l)}(t) \rho_e^{(l,k)}(t)), \\
 \text{s. t.} \quad & (z, \lambda, \mu, \nu, \eta) \in \Phi(x^{(k)}).
 \end{aligned}$$

Note that **(LBP<sub>k</sub>)** is a linear program and much easier to solve than the non-convex Problem **(P4)**. Let  $\text{obj}_k$  denote the optimal objective value of **(LBP<sub>k</sub>)**. If Problem **(LBP<sub>k</sub>)** is solved to optimum with a finite  $\text{obj}_k$ , we will then obtain a feasible solution of **(P4)** with speed limit  $u^{(k)} := \sum_{i \in \mathcal{O}} \gamma^{(i)} x_i^{(k)}$  and certificate  $\hat{J}(u^{(k)}) := \text{obj}_k$ ; otherwise, Problem **(LBP<sub>k</sub>)** is either infeasible or unbounded, i.e.,  $\text{obj}_k = -\infty$ . The lower bound of **(P4)** can be calculated by  $\text{LB}_k = \max_{p=1, \dots, k} \{\text{obj}_p\}$ . The stopping criterion of the algorithm can be determined by one of the following criteria

- 1)  $\text{UB}_k - \text{LB}_k \leq \epsilon$ ,
- 2) **(UBP<sub>k</sub>)** is infeasible,
- 3) A satisfactory sub-optimal solution is found after certain running time  $T_{\text{run}}$ .

In [57], it is shown that such algorithms convergence to a global  $\epsilon$ -optimal solution after finite number of iterations when we use the first and second stopping criteria. The third solution criterion allow us to find a potentially good performance-guaranteed feasible solution within certain running time  $T_{\text{run}}$ .

**Remark V.2 (Online tractable solutions to (P4))** The data-driven control requires to solve a sequence of **(P4)** online. We achieve this by an online ‘‘warm start’’ of Algorithm 2, which employs an assimilation set  $\mathcal{I}_t := \{u^{(s)}\}_s$  that contains the historically-generated speed-limit candidates, where  $s$  indexes these candidates. In particular, at each time solving a problem **(P4)**, the candidates in  $\mathcal{I}_t$  can be explored by the solution to **(LBP<sub>k</sub>)** of each  $u^{(s)} \in \mathcal{I}_t$ . Notice that these **(LBP<sub>k</sub>)** can be executed in parallel. Then, these examined candidates contribute to integer cuts in **(UBP<sub>k</sub>)** when executing Algorithm 2. At the termination of the current **(P4)**, a new set of candidates are updated to  $\mathcal{I}_{t+1}$  for later evaluation of **(P4)**.

## VI. ANALYSIS VIA SECOND-ORDER CONE PROBLEMS

This section provides a tool to analyze the efficacy of the proposed algorithm for the nonconvex Problem **(P4)**. In particular, we propose a second-order cone relaxation for the non-convex quadratic terms  $\{\nu^{(l)} \circ \rho^{(l)}\}_{l \in \mathcal{L}}$  in **(P4)**, and a second-order cone relaxation for it. We then present the conditions under which this convex relaxation is exact. To enable the tool for analysis, we assume the following:

<sup>9</sup>Given  $u^{(k)}$  and  $\{\rho^{(l,k)}\}_{l \in \mathcal{L}}$ , the equivalent dual of **(LBP<sub>k</sub>)** is

$$\begin{aligned}
 \min_{\rho^{(l)}, l \in \mathcal{L}} \quad & \frac{1}{NT} \sum_{e, t, l} u_e^{(k)}(t) \rho_e^{(l)}(t) \\
 \text{s. t.} \quad & 0 \leq \rho^{(l)} \leq \rho^c(u^{(k)}), \forall l \in \mathcal{L}, \\
 & \sum_{l \in \mathcal{L}} \|\rho^{(l)} - \rho^{(l,k)}\| \leq \epsilon(\beta),
 \end{aligned}$$

which results in more efficient online solutions.

**Assumption VI.1 (Highway densities are nontrivial)** For all  $e \in \mathcal{E}$ ,  $t \in \mathcal{T}$  and  $l \in \mathcal{L}$ , we assume  $\rho_e^{(l)}(t) \geq \epsilon(\beta)$ , where the parameter  $\epsilon(\beta)$  is the radius of the Wasserstein ball.

**Remark VI.1 (On nontrivial highway densities)** Assumption VI.1 depends on the radius of the Wasserstein ball, which is selected as in Remark III.2. In reality, we could select the value  $\epsilon(\beta)$  to be sufficiently small, even if it potentially sacrifices confidence on performance guarantees. In any case, there are three cases to consider: 1) the density on each segment of highway is just zero, 2) there are zero density values  $\rho_e^{(l)}(t)$ , for some  $(e, t, l)$ , while the rest of  $\rho_e^{(l)}(t)$  are upper bounded by a value that is smaller than the maximal critical density  $\max_{u \in \Gamma} \rho_e^c(u_e(t))$ , and 3) there are some values  $\rho_e^{(l)}(t)$  that go beyond the maximal critical density, e.g.,  $\rho_e^{(l)}(t) > \epsilon(\beta) + \arg\max_{u \in \Gamma} \rho_e^c(u)$ . In the first case, no congestion would happen and there is no need for speed-limit control. The second case can be handled by tuning  $\epsilon(\beta)$  to be small enough. In the third case, with a given small  $\epsilon(\beta)$ , there is already congestion on some segment of the highway and no feasible speed limit would eliminate that congestion.

Assumption VI.1 enables us to explore properties of the optimizers of (P4) as in the following proposition.

**Proposition VI.1 (Optimizers in a cone)** Let  $\text{sol}^* := (x^*, y^*, z^*, \rho^*, \lambda^*, \mu^*, \nu^*, \eta^*)$  be any optimizer of Problem (P4). If Assumption VI.1 holds, we have  $\nu^* \circ \rho^* \geq \mathbf{0}_{nTN}$ .

Proposition VI.1 allows us to explore structure of the bi-linear terms  $\{\nu^{(l)} \circ \rho^{(l)}\}_{l \in \mathcal{L}}$  via second-order cone constraints. This is achieved by introducing variables  $\vartheta_e^{(l)}(t)$  and writing Problem (P4) as follows

$$\begin{aligned}
 (\text{P4}') \quad & \max_{\substack{x, y, z, \rho, \\ \lambda, \mu, \nu, \eta, \vartheta}} -\lambda\epsilon(\beta) - \frac{1}{N} \sum_{e, t, l} \bar{f}_e \bar{\rho}_e \eta_e^{(l)}(t) + \frac{1}{N} \sum_{e, t, l} (\vartheta_e^{(l)}(t))^2, \\
 \text{s. t.} \quad & \vartheta^2 \leq \nu \circ \rho, \\
 & \text{speed limits (11), sample trajectories \{(15), (16)\},} \\
 & \text{no congestion \{(14), (17), (18), (19), (20)\}.}
 \end{aligned} \tag{23}$$

For each  $e \in \mathcal{E}$ ,  $t \in \mathcal{T}$  and  $l \in \mathcal{L}$ , the constraint (23) can be equivalently written as the following second-order cone:

$$\sqrt{(\nu_e^{(l)}(t))^2 + (\rho_e^{(l)}(t))^2 + 2(\vartheta_e^{(l)}(t))^2} \leq \nu_e^{(l)}(t) + \rho_e^{(l)}(t). \tag{24}$$

Problem (P4) and (P4') are equivalent as the following:

**Lemma VI.1 (Equivalent optimizer sets of (P4) and (P4'))** Problem (P4') is equivalent to (P4) in the sense that their optimal objective values are the same and the set of optimizer of (P4) is the projection of that of (P4'). Further, any feasible solution of (P4') can give us a valid performance guarantee (9) with certificate to be objective function of (P4') evaluated at that feasible solution.

Problem (P4') is still non-convex. To approximate the quadratic terms in the objective, we will first show that variables  $\vartheta_e^{(l)}(t)$  are bounded.

**Lemma VI.2 (Bounded variable  $\vartheta$ )** *Let Assumption IV.1 on bounded  $\eta$  hold, then there exists large enough scalar  $\bar{\vartheta}$  such that  $|\vartheta_e^{(l)}(t)| \leq \bar{\vartheta}$  for all  $e \in \mathcal{E}$ ,  $t \in \mathcal{T}$  and  $l \in \mathcal{L}$ .*

Lemma VI.2 enables us to approximate each component of  $\vartheta$  by a finite set of points within its range. Let (sufficiently large)  $K$  denote the number of points and let us denote the set of these points by  $Q := \{\pi_1, \dots, \pi_K\} \subset \mathbb{R}$ . We use the set  $\mathcal{Q} := \{1, \dots, K\}$  to index these points. For each edge  $e \in \mathcal{E}$ , time  $t \in \mathcal{T}$  and sample  $l \in \mathcal{L}$ , let us define the binary variable  $q_{e,k}^{(l)}(t)$  to be equal to one if  $\vartheta_e^{(l)}(t)$  is approximated by  $\pi_k$ ; otherwise  $q_{e,k}^{(l)}(t) = 0$ . Then for each  $e \in \mathcal{E}$ ,  $t \in \mathcal{T}$  and  $l \in \mathcal{L}$ , we will then represent  $\vartheta_e^{(l)}(t)$  by the following constraints

$$\begin{aligned} \vartheta_e^{(l)}(t) &= \sum_{k \in \mathcal{Q}} \pi_k q_{e,k}^{(l)}(t), & \sum_{k \in \mathcal{Q}} q_{e,k}^{(l)}(t) &= 1, \\ & \forall e \in \mathcal{E}, t \in \mathcal{T}, l \in \mathcal{L}, \\ q_{e,k}^{(l)}(t) &\in \{0, 1\}, \forall e \in \mathcal{E}, t \in \mathcal{T}, l \in \mathcal{L}, k \in \mathcal{Q}. \end{aligned} \tag{25}$$

Using this representation, we find approximated solutions of (P4') by solving the following

$$\begin{aligned} \text{(P5)} \quad & \max_{\substack{x,q,y,z,\rho, \\ \lambda,\mu,\nu,\eta,\vartheta}} -\lambda\epsilon(\beta) - \frac{1}{N} \sum_{e,t,l} \bar{f}_e \bar{\rho}_e \eta_e^{(l)}(t) \\ & + \frac{1}{N} \sum_{e,t,l,k} (\pi_k)^2 q_{e,k}^{(l)}(t), \end{aligned}$$

s. t. **level approximation** (25), **second-order cone** (24),  
**speed limits** (11), **sample trajectories** {(15), (16)},  
**no congestion** {(14), (17), (18), (19), (20)}.

Problem (P5) is an SOCMIP and can be solved to optimum by commercial solvers, such as GUROBI and MOSEK. Note that for any feasible solution of (P5), it is feasible for (P4') and its objective value is a valid lower bound for that of (P4'). Thus, any feasible solution of (P5) together with its objective value provide performance guarantees (9) via Lemma VI.1. Further, as the number of partition points  $K \rightarrow \infty$ , Problem (P5) is computationally equivalent to Problem (P4'), and therefore the same as Problem (P4). Notice that online solutions to Problem (P5) are inaccessible and (P5) serves as a tool for the performance analysis of the proposed algorithm. In the following section, we leverage this tool to analyze the performance of the algorithm in an academic example.

## VII. SIMULATIONS

In this section, we demonstrate in an example how to efficiently find a solution to (P4) that results in a robust data-driven variable-speed limit  $u$  with performance guarantee (9). The analysis of the results are twofold. First, we verify the effectiveness of the proposed integer solution search algorithm by comparing it with the monolith approach that solves an approximation to (P4), Problem (P5). Second, to verify the robustness of the solution and performance guarantees in probability, we compare the resulting distributionally robust data-driven control with the control obtained from the sample-averaged optimization problem. Both controls are applied on a naive highway simulator developed via the standard cell transmission model [44].

**Simulation setting:** We consider an 8-lane highway with length  $L = 10\text{km}$  and we divide it into  $n = 5$  segments with equal length. Let the unit size of each time slot  $\delta = 30\text{sec}$  and consider  $T = 20$  time slots for a 10min planning horizon. For each edge  $e \in \mathcal{E}$ , we propose a traffic jam density of  $\bar{\rho}_e = 1050\text{vec/km}$ , a capacity of  $\bar{f}_e = 3.1 \times 10^4\text{vec/h}$ <sup>10</sup> and a maximal speed limit of  $\bar{u}_e = 140\text{km/h}$ . Let us consider  $m = 5$  different candidate speed limits  $\Gamma = \{40\text{km/h}, 60\text{km/h}, 80\text{km/h}, 100\text{km/h}, 120\text{km/h}\}$ . On the 4<sup>th</sup> edge  $e := (3, 4) \in \mathcal{E}$ , we assume an accident happens during  $\mathcal{T}$  with parameters  $\bar{f}_e = 2.7 \times 10^4\text{vec/h}$ . To evaluate the effect of the proposed algorithm, samples of the random variables  $\rho(0)$ ,  $w$ ,  $r^{\text{in}}$  and  $r^{\text{o}}$  are needed. In real-case studies, samples  $\{\rho^{(l)}(0)\}_{l \in \mathcal{L}}$  can be obtained from highway sensors (loop detectors), while samples of the uncertain mainstream flows  $\{\omega^{(l)}\}_{l \in \mathcal{L}}$  and flow fractions  $\{r^{\text{in},(l)}, r^{\text{o},(l)}\}_{l \in \mathcal{L}}$  can be constructed either from a database of flow data on the highway, or from the current measurements of ramp flows with the assumption that the stochastic process  $\{\omega(t), r^{\text{in}}(t), r^{\text{o}}(t)\}_{t \in \mathcal{T}}$  is trend stationary.

**Fictitious datasets:** In this simulation example, the index set of accessible samples is given by  $\mathcal{L} = \{1, 2, 3\}$ . For each  $l \in \mathcal{L}$ , let us assume that each segment  $e \in \mathcal{E}$  initially operates under a free flow condition with an initial density  $\rho_e^{(l)}(0) = 260\text{vec/km}$ . To ensure significant inflows of the system, we let the samples  $\{\omega^{(l)}(t)\}_{l \in \mathcal{L}, t \in \mathcal{T}}$  of the mainstream inflow to be chosen from the uniform distribution within interval  $[2 \times 10^4, 2.4 \times 10^4]\text{vec/h}$ . For each edge  $e \in \mathcal{E}$  and time  $t \in \mathcal{T}$ , we further assume that samples  $\{r^{\text{in},(l)}(t)\}_{l \in \mathcal{L}}$  and  $\{r^{\text{o},(l)}(t)\}_{l \in \mathcal{L}}$  are generated from uniform distributions within interval  $[0, 5\%]$  and  $[0, 3\%]$ , respectively. We also let the confidence value be  $\beta = 0.05$  and the radius of the Wasserstein Ball  $\epsilon(\beta) = 0.985$  as calculated in [60].

**Effectiveness of the algorithm:** To generate feasible solutions that can be carried out for a real time transportation system, we allocate  $T_{\text{run}} = 1\text{min}$  execution time for control design and run algorithms on a machine with two core 1.8GHz CPU and 8G RAM. In this allocated 1 minute, we consider the speed limit design in 2 approaches: 1) we run the proposed Algorithm 2 to solutions of the Problem (P4), and 2) we run optimization solver MOSEK to solutions of the monolith Problem (P5). The partition number  $K = 5$  is selected for the monolith approach.

We present in Table I the comparison of the mentioned two approaches. In 1 minute, the Algorithm 2 executed 19 candidate speed limits where 2 feasible speed limits were found at time 6.7sec and 28.7sec. We verified that  $\hat{J}(u^{(2)}) = 1.17 \times 10^5\text{vec/h}$  is the highest certificate obtained, i.e.,  $\hat{J}(u^{(2)}) \in \arg\max_{p=1,2} \{\hat{J}(u^{(p)}) \mid u^{(p)} \text{ is feasible}\}$ , and the desired speed limits are

$$u^{(2)} = [120, 100, 80, 80, 100]\text{km/h}.$$

Compared with the proposed algorithm, the monolith approach returned a feasible solution with the speed limits  $u^{\text{mon}} = [120, 120, 120, 40, 40]\text{km/h}$  and an approximated throughput  $3.93 \times 10^4\text{vec/h}$ . It can be seen that 1) the gap (difference between UB and LB) obtained from the Algorithm 2 is tighter than that obtained from the monolith approach, and 2) the implementable speed limits proposed by the Algorithm 2 results in higher throughput than that achieved by the monolith.

In the following subsection, we use the speed limits  $u^{(2)}$  to verify the guarantees on congestion elimination with high probability.

**Distributionally robust decisions:** To demonstrate the distributional robustness of our approach, we compare the performance of our speed limits design  $u^{(2)}$  with the performance of the speed limits developed from a sample average optimization problem, which is also known as the dual

<sup>10</sup>The unit ‘‘vec’’ stands for ‘‘vehicles’’. Notice the proposed capacity is about 50% higher than the actually highway capacity in order to leverage the actual fundamental diagram for control.

	Algorithm 2 <sup>a</sup>	Monolith
# of feasible cand. <sup>b</sup>	2	1
# of infeasible cand.	17	NA
LB (vec/h)	$1.17 \times 10^5$	$3.93 \times 10^4$
UB (vec/h)	$1.55 \times 10^5$	$1.55 \times 10^5$

<sup>a</sup>: Subproblems (UBP<sub>k</sub>) and (LBP<sub>k</sub>) are solved via MOSEK.

<sup>b</sup>: Candidate speed limit.

TABLE I: The efficiency of the proposed Algorithm 2.

version of the scenario-based approach, such as in [45]. In particular, the sample averaged version of (P) (equivalently, (P1)) is the one substitutes the unknown distribution  $\mathbb{P}(u)$  with its empirical distribution  $\hat{\mathbb{P}}(u)$ . The resulting tractable formulation of the sample average problem, analogous to (P4), is the following

$$\begin{aligned}
& \max_{\substack{x,y,z,\rho, \\ \mu,\nu,\eta}} - \frac{1}{N} \sum_{e,t,l} \bar{f}_e \bar{\rho}_e \eta_e^{(l)}(t) + \frac{1}{N} \sum_{e,t,l} \nu_e^{(l)}(t) \rho_e^{(l)}(t), \\
\text{s. t. } & \sum_{i \in \mathcal{O}} \gamma^{(i)}(\bar{\rho} - \rho^c(\bar{u})) \otimes \mathbf{1}_T \circ z_i^{(l)} - \mu^{(l)} \\
& \quad + \bar{f} \otimes \mathbf{1}_T \circ \eta^{(l)} \geq \mathbf{0}_{nT}, \forall l \in \mathcal{L}, \\
& \nu^{(l)} = \mu^{(l)} + \frac{1}{T} \sum_{i \in \mathcal{O}} \gamma^{(i)} x_i, \forall l \in \mathcal{L}, \\
& \mathbf{0}_{nT} \leq \eta^{(l)} \leq \bar{\eta}, \forall l \in \mathcal{L}, \\
& \text{speed limits (11), dual variable (14),} \\
& \text{sample trajectories}\{(15), (16)\}.
\end{aligned}$$

Note that the difference between the previous sample average problem and (P4) is that the former has a Wasserstein Ball radius  $\epsilon(\beta) = 0$  and, thus, unlike (P4), it does not provide a performance guarantee on congestion. We solve the above sample average problem to a suboptimal solution via the Algorithm 2 with the same setting as in solution to  $u^{(2)}$ . The resulting speed limit design is the following

$$u^{\text{sav}} = [60, 60, 80, 60, 100] \text{km/h.}$$

To verify the performance of  $u^{(2)}$  and  $u^{\text{sav}}$ , we generated  $N_{\text{val}} = 10^3$  validation samples of random variables  $\rho(0)$ ,  $w$ ,  $r^{\text{in}}$  and  $r^{\text{o}}$  that are from the distributions described in the Fictitious datasets paragraph. The speed limit design  $u^{(2)}$ ,  $u^{\text{sav}}$  as well as the validation dataset are integrated into a highway simulator with the highway parameter settings described in the Simulation setting paragraph.

Due to space limitations we cannot showcase all admissible sample trajectories for  $10^3$  scenarios, therefore in Fig. 4 we show an average of the admissible sample trajectories, i.e., the function  $\frac{1}{N_{\text{val}}} \sum_{l \in \{1, \dots, N_{\text{val}}\}} \rho_e^{(l)}(t)$  for each segment  $e$ , with speed limits  $u^{(2)}$  and  $u^{\text{sav}}$ , and present an arbitrarily chosen scenario 638 in Fig. 5. We select the simulation time horizon to be twice of that the planning horizon's in order to see the effect of the design clearly. We verified that the density evolution under speed limits  $u^{(2)}$ , and, in particular, the density trajectory of

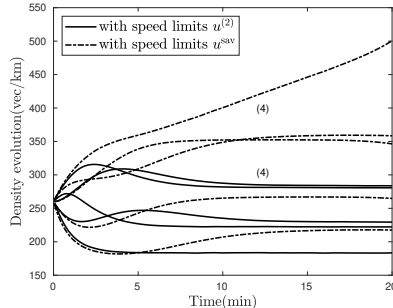


Fig. 4: Density evolution of each segment  $e$ , with speed limits  $u^{(2)}$  and  $u^{\text{sav}}$ . Each trajectory corresponds to a segment  $e \in \{(1), (2), \dots, (5)\}$ . For simplicity we only label segment (4), which happens to have an accident during the planning horizon.

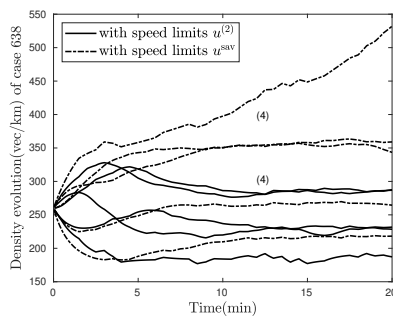


Fig. 5: A representative density evolution of segments, with speed limits  $u^{(2)}$  and  $u^{\text{sav}}$ . The sample 638 was arbitrarily chosen for demonstration purpose.

accident edge (4), did not exceed the critical density values ( $\rho_4^c(80\text{km/h}) = 335\text{vec/km}$ ) for each sample. Thus the highway  $\mathcal{G}$  is kept free of congestion in this planning horizon  $\mathcal{T}$  with high probability. However, the same robust behavior can not be guaranteed under speed limits  $u^{\text{sav}}$ , as vehicles accumulate significantly on edge (4) for too many samples (contrast to its critical density  $\rho_4^c(60\text{km/h}) = 403\text{vec/km}$ ), see Fig. 4. We claim the robustness of our design compared to the design from sample average problem, as the latter does not ensure such out-of-sample performance guarantees.

## VIII. SIMULATION STUDY

In this section, we illustrate the proposed data-driven speed-limit control on a highway system located in San Diego, California, USA. The purpose of this simulation is to show the good behavior of the proposed method under uncertainty as compared with that of the current traffic speed limits on the highway. While this is a first good indication, more work would be required to assess the behavior of the method over different traffic indices. However, our main focus is the theoretical development of the algorithm itself and so these questions are left for future work.

**Highway system:** We selected a highway section from Encinitas to Del Mar on the I-5 San Diego Freeway with length  $L \approx 11$  km, as shown in Fig. 6. The highway was divided into  $n = 26$  segments with various lengths  $\{\text{len}_e\}_{e \in \mathcal{E}}$  ranging from 200 m to 2 km. These segments have a number of lanes  $\{\text{lane}_e\}_{e \in \mathcal{E}}$  ranging from 4 to 8, and there are 7 on-ramps and 5 off-ramps

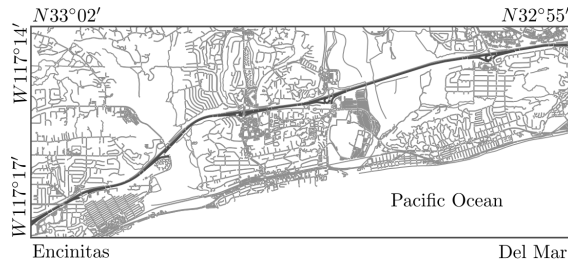


Fig. 6: Highway section from Encinitas to Del Mar, San Diego, US.

distributed on the highway. We obtained real-time traffic data with 30 seconds precision from the California Highway Performance Measurement System (PeMS), and used it to reproduce the actual traffic flow features via the software Simulation of Urban MObility (SUMO) [61], which is a microscopic and continuous traffic simulation package. We calibrated the simulator using PeMS data which were collected between 12pm and 2pm on a particular day, and the speed limit on San Diego Freeway was 105 km/h or 65 mph.

**Data-driven control:** The data-driven control to solve (P) considered  $T = 80$  time slots dividing 4-minutes planning horizon, with a unit size of each time slot  $\delta = 3$  seconds. The infrastructure-related parameters ( $n, L, \text{len}, \text{lane}$ ) were selected to be the same as that of the highway system, only that ramp-related ultra-short lanes were excluded. We considered  $m = 6$  different candidate speed limits  $\Gamma = \{30, 50, 70, 90, 110, 130\}$  (km/h). The control  $u$  was obtained by implementing Algorithm 2 that solves the equivalent (P4), taking a  $T_{\text{run}} = 1$  minute and executing Algorithm 2 every 2 minutes. To achieve realistic driving instructions, we added extra speed limit constraints to ensure constant  $u$  over each 1 minute interval.

**System monitor:** We assume the existence of a system monitor which provides information of the real-time traffic flow data  $\{\varpi^{(l)}\}_{l \in \mathcal{L}}$  as well as the random events parameters  $(\bar{f}, \bar{\rho}, \bar{u})$ . Practically, these parameters can be calibrated in advance from PeMS historical data. In particular, at each time when Algorithm 2 is to be executed, we consider  $N = 2$  accessible samples with the set  $\mathcal{L} = \{1, 2\}$ . Precisely, values of  $\varpi^{(1)}$  were constructed and propagated using real-time highway sensor measurements (loop detectors data in PeMS) and values of  $\varpi^{(2)}$  were obtained as the 7-day average data corresponding to the same time period (12pm to 2pm). This results in a radius for the Wasserstein Ball  $\epsilon(\beta) \approx 5$ , given the confidence value  $\beta = 0.05$ . Notice that more samples can be added to reduce the radius if various source of measurements are accessible, e.g., such as real-time GPS data. On the other hand, the infrastructure and event-related data  $\{\bar{f}_e, \bar{\rho}_e, \bar{u}_e\}_{e \in \mathcal{E}}$  are determined theoretically, where values  $\{\bar{f}_e\}_{e \in \mathcal{E}}$  have range  $[1.1, 2.3] \times 10^4$  (vec/h),  $\{\bar{\rho}_e\}_{e \in \mathcal{E}}$  with values in  $[0.5, 1] \times 10^3$  (vec/km/edge), and  $\{\bar{u}_e\}_{e \in \mathcal{E}}$  are assumed 200 (km/h).

**Benchmarks:** We consider a 2-hour scenario, from 12pm to 2pm, and assume a temporary lane closure on the 15<sup>th</sup> segment between 1pm to 1 : 20pm, which introduces a capacity and jam density drop by 35% on that particular segment, located at 4.5 km from the entry. Further, we implement the proposed data-driven control between 12 : 30pm to 2pm, and compare the resulting performance with that of the highway system without control, i.e., with constant speed limit 105 km/h. Notice that, if congestion is inevitable, namely, the data-driven control problem (P) is infeasible under the admissible regime, we implement the default speed limit (105 km/h) instead.

**Performance analysis:** Fig. 7 shows the traffic density profile in time and space, where the origin indicates the entry of the highway at the initial time, i.e., Encinitas at time 12pm. The x-axis indicates the time (number of hours) passed from 12pm and the y-axis is the distance to



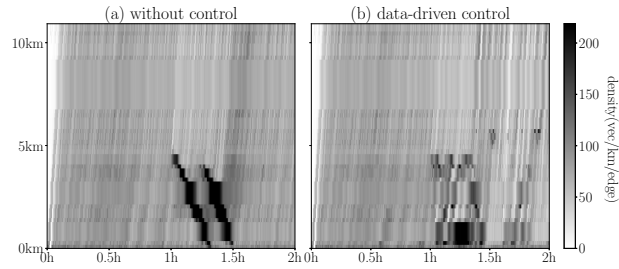


Fig. 7: Time-space profile of traffic average density.

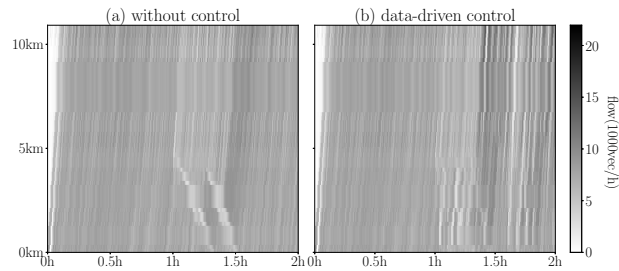


Fig. 8: Time-space profile of traffic average flow.

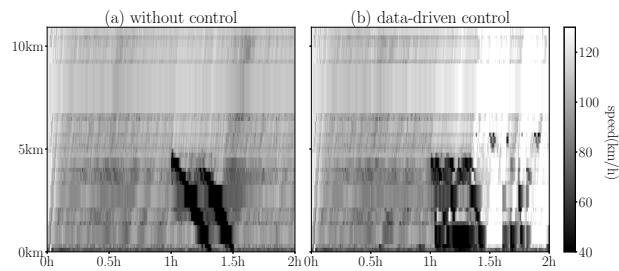


Fig. 9: Time-space profile of traffic average speed.

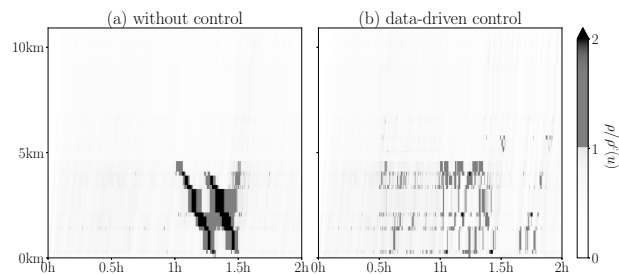


Fig. 10: Time-space profile of congestion ratio  $\rho(t)/\rho^c(u(t))$ .

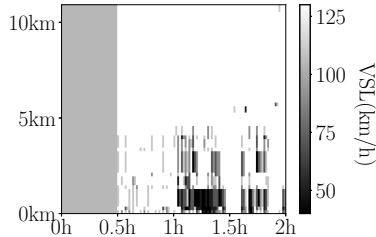


Fig. 11: Time-space profile of speed limits  $u(t)$ .

the highway entry. Similarly, Fig. 8 and Fig. 9 demonstrate the flow and average speed profiles of those, respectively. For comparison, subfigures (a) are profiles without control and subfigures (b) are those with the data-driven control. It can be observed that, during the period 0h to 0.5h (12pm to 12 : 30pm), the two profiles were statistically identical. During period 0.5h to 1h (12 : 30pm to 1pm), as the mainstream flows were moderate, the speed-limit control assigned a higher speed limit (130 km/h) than the default 105 km/h on the majority of the segments. See Fig. 11 for the speed limit profile. After 1h (1pm), a significant capacity drop occurs on the middle of the highway due to a temporary lane closure. This event leads to congestion on the preceding segment and backward congestion waves start to transmit on the highway, see, e.g., subfigures (a). The darker parts on the profiles indicate congestion and notice how the congestion was transmitted to the entry of the highway over time. In addition, during the lane closure period (1pm to 1 : 20pm), the data-driven control then took effect to cancel/reducing the congestion transmission by dynamically assigning low speed limits on the upper stream of the highway. See, e.g., Fig. 11 on the speed limit assignment during 1h to 1.4h, which regulates the highway average speed as in Fig. 9(b). These actions eliminated the congestion waves and reduced the effect of the random events. See, e.g., Fig. 7 and 8 for comparison of the effect of the congestion elimination, Fig. 10 for the significant reduction of the congestion ratio  $\rho(t)/\rho^c(t)$ , and Fig. 11 for the assignment of the variable speed limit. When the random event ended, the speed-limit control then resumed to normal operation, which, during 1.4h to 2h, dynamically assigned speed limits to account for uncertainties on random ramp flows. See, e.g., the scattered speed restrictions in Fig. 11. Furthermore, notice in Fig. 10(b) how the actual highway density  $\rho(t)$  violated the prediction-and-assignment critical density  $\rho^c(u)$  via speed limits  $u$ . These are the original driving forces to update speed limits. Notice that, during this whole scenario, the data-driven control problem (P) is feasible. Otherwise, the speed limit would be set to the default 105 km/h at some time later than 0.5h in Fig. 11. This indicates a successful containment of the congestion. When the congestion is too heavy, (P) could be infeasible for some time period due to the extreme-high density on some of the segments. In those scenarios, to handle the congestion, small enough candidates can be added to the candidate speed limit set  $\Gamma$  in order for larger, admissible operation zone of (P). Otherwise, the congestion is inevitable as (P) is infeasible, and we simply select the default, pre-selected speed limits. At last, notice that the control performance relies heavily on the selection of the objective function of (P) as well as on the available information on the flow and random events data. We leave the questions regarding other traffic performance metrics and the improvement of the controller employing more accurate traffic models for the future work.

## IX. CONCLUSIONS

In this paper, we formulate a data-driven predictive control problem with probabilistic performance guarantees as a distributionally optimization problem. We equivalently reformulate this intractable Problem (P) into a non-convex but tractable Problem (P4), or Mixed Integer Second Order Cone Problem (P5). This is achieved by: 1) extending Distributionally Robust Optimization theory to account for system dynamics; 2) reformulation and relaxation techniques. Finally, we adapt the idea of decomposition and propose an integer-solution search algorithm for efficient solutions of Problem (P4), or commercial solvers for that of Problem (P5). The proposed approaches provide performance guarantee (8) for Problem (P). To explicitly demonstrate the proposed approach, we consider a highway speed-limit control problem that accounts for random inflows, outflows and events. Finally, we demonstrate the theoretical effectiveness of this work via simulations. In particular, we simulated traffic flows on a highway in San Diego, and show the effectiveness of the designed speed limits numerically.

## APPENDIX

**Proof of Lemma III.1:** Continuous functions of i.i.d. random variables generate i.i.d. random variables. Thus, the admissible sample trajectories  $\{\rho^{(l)}\}_{l \in \mathcal{L}}$  generated by (10) are i.i.d. realizations of  $\mathbb{P}(u)$ . ■

**Proof of Lemma III.2:** The proof consists of two steps. First, we explore the boundedness property of  $\rho_e(t)$  w.r.t.  $\varpi$ , for all  $e \in \mathcal{E}$  and  $t \in \mathcal{T}$ . Second, we claim that there exists an  $a > 1$  such that  $\mathbb{E}_{\mathbb{P}(u)}[\exp(\|\rho\|^a)] < \infty$ .

**Step 1: (Boundedness of  $\rho$ )** Consider for each speed limit  $u$  and time  $t \in \mathcal{T} \setminus \{0\}$ . Let  $A(u, t)$  denote the matrix that is consistent with the highway system  $\mathcal{G}$ , let  $B(t)$  denote the column vector that encodes the mainstream flow  $\omega$ , and write the density  $\rho(t)$  in the following compact form

$$\rho(t) = \Phi(t, 0)\rho(0) + \sum_{\tau=0}^{t-1} \Phi(t, \tau + 1)B(\tau),$$

where

$$\Phi(t, \tau) := \begin{cases} I_n, & \text{if } t = \tau, \\ A(u, t-1)A(u, t-2) \cdots A(u, \tau), & \text{if } t > \tau, \end{cases}$$

$$A(u, t) = \begin{bmatrix} m_1(t) & & & & \\ n_1(t) & \ddots & & & \\ & \ddots & \ddots & & \\ & & \ddots & \ddots & \\ & & & n_{n-1}(t) & m_n(t) \end{bmatrix}, B(t) = \begin{bmatrix} h_{(0,1)}\omega(t) \\ 0 \\ \vdots \\ 0 \end{bmatrix},$$

with

$$m_i(t) = 1 - h_e u_e(t), \quad \forall i \in \{1, \dots, n\}, e = (i-1, i),$$

$$n_j(t) = \min \left\{ \frac{1 - r_s^o(t)}{1 - r_e^{\text{in}}(t)} h_e u_s(t), \frac{\bar{f}_e}{\rho_s(t)}, \tau_e \bar{u}_e \frac{\bar{p}_e - \rho_e(t)}{\rho_s(t)} \right\},$$

$$\forall j \in \{1, \dots, n-1\}, s = (i-1, i), e = (i, i+1).$$

Given that each component of  $A(u, t)$  is bounded for fixed  $u$  and  $t$ , the induced norm of  $A(u, t)$  is also bounded and we denote their universal bound by  $A_0$ . Similarly, we denote by

$\bar{h}$  the upper bound on  $h_e$ ,  $e \in \mathcal{E}$ . Then for every  $t$  we can bound the infinity norm of  $\rho(t)$  as follows

$$\begin{aligned} \|\rho(t)\|_\infty &\leq \|\Phi(t, 0)\|_\infty \|\rho(0)\|_\infty \\ &\quad + \bar{h} \sum_{\tau=0}^{t-1} \|\Phi(t, \tau+1)\|_\infty \|\omega(\tau)\|_\infty, \\ &\leq A_0^t \|\rho(0)\|_\infty + \bar{h} \sum_{\tau=0}^{t-1} A_0^{t-\tau-1} \|\omega(\tau)\|_\infty, \\ &\leq M_1(t) \left( \|\rho(0)\|_\infty + \sum_{\tau=0}^{t-1} \|\omega(\tau)\|_\infty \right), \\ &\leq (t+1)M_1(t)\|\varpi\|_\infty, \leq (t+1)M_1(t)\|\varpi\|, \end{aligned}$$

where  $M_1(t) := \max\{A_0^t, \bar{h}, \bar{h}A_0^t\}$ .

**Step 2: (Light-tailed distribution)** Given an  $u$ , consider a time  $t^* \in \operatorname{argmax}_{t \in \mathcal{T} \setminus \{0\}} \{\|\rho(t)\|_\infty\}$ . Then by norm equivalence we have

$$\begin{aligned} \|\rho\| &\leq n\|\rho\|_\infty = n \max_{t \in \mathcal{T} \setminus \{0\}} \{\|\rho(t)\|_\infty\}, \\ &= n\|\rho(t^*)\|_\infty, \leq n(t^*+1)M_1(t^*)\|\varpi\|. \end{aligned}$$

Then for any  $a > 1$  with  $\mathbb{E}_{\mathbb{P}_\varpi}[\exp(\|\varpi\|^a)] < \infty$ , let  $M_2 = [n(t^*+1)M_1(t^*)]^a < \infty$  and we have

$$\begin{aligned} \mathbb{E}_{\mathbb{P}(u)}[\exp(\|\rho\|^a)] &\leq \mathbb{E}_{\mathbb{P}_\varpi}[\exp(M_2\|\varpi\|^a)], \\ &= \exp(M_2)^a \cdot \mathbb{E}_{\mathbb{P}_\varpi}[\exp(\|\varpi\|^a)] < \infty. \end{aligned}$$

That is,  $\mathbb{P}(u)$  is light tailed. ■

**Proof of Theorem III.1:** We prove the result in two steps. First, we show the proposed set  $\mathcal{P}(u)$  contains the unknown distribution  $\mathbb{P}(u)$  with high probability. Then, we show that the proposed certificate  $J(u)$  provides performance guarantees as in (9).

**Step 1: (Tractable set containing  $\mathbb{P}(u)$ )** Under Assumption III.1 and using  $N$  i.i.d. samples of  $\varpi$ , we obtain i.i.d. samples  $\{\rho^{(l)}\}_{l \in \mathcal{L}}$  of  $\mathbb{P}(u)$  via Lemma III.1. Then, with the distribution

$$\hat{\mathbb{P}}(u) := \frac{1}{N} \sum_{l \in \mathcal{L}} \delta_{\{\rho^{(l)}\}},$$

we quantify the relation between  $\hat{\mathbb{P}}(u)$  and  $\mathbb{P}(u)$  via Lemma III.2 and the following theorem:

**Theorem A.1 (Measure concentration [62, Theorem 2])** *If  $\mathbb{P}(u) \in \mathcal{M}_\ell(\mathcal{Z}(u))$ , then*

$$\operatorname{Prob}^N \{d_W(\mathbb{P}(u), \hat{\mathbb{P}}(u)) > \epsilon\} < \begin{cases} c_1 e^{-c_2 N \epsilon^{\max\{2, \ell\}}}, & \text{if } \epsilon \leq 1, \\ c_1 e^{-c_2 N \epsilon^a}, & \text{if } \epsilon > 1, \end{cases}$$

for all  $N \geq 1$ ,  $\ell \neq 2$ , and  $\epsilon > 0$ , where the parameter  $\ell$  is the dimension of  $\rho$ , and parameters  $c_1, c_2$  are positive constants that only depend on  $\ell, a$  and  $b$  as in Assumption III.1. □

Let us select  $\epsilon := \epsilon(\beta)$  to be the following

$$\epsilon(\beta) := \begin{cases} \left( \frac{\log(c_1 \beta^{-1})}{c_2 N} \right)^{1/\max\{2, \ell\}}, & \text{if } N \geq \frac{\log(c_1 \beta^{-1})}{c_2}, \\ \left( \frac{\log(c_1 \beta^{-1})}{c_2 N} \right)^{1/a}, & \text{if } N < \frac{\log(c_1 \beta^{-1})}{c_2}, \end{cases}$$

then Theorem **A.1** leads to

$$\text{Prob}^N \left( d_W(\mathbb{P}(u), \hat{\mathbb{P}}(u)) > \epsilon(\beta) \right) < \beta,$$

or, equivalently,

$$\text{Prob}^N \left( d_W(\mathbb{P}(u), \hat{\mathbb{P}}(u)) \leq \epsilon(\beta) \right) \geq 1 - \beta.$$

From the definition of the Wasserstein ball  $\mathbb{B}_{\epsilon(\beta)}(\hat{\mathbb{P}}(u))$  and the fact that  $\mathbb{P}(u) \in \mathcal{M}_{\text{It}}(\mathcal{Z}(u))$ , we have

$$\text{Prob}^N \left( \mathbb{P}(u) \in \mathbb{B}_{\epsilon(\beta)}(\hat{\mathbb{P}}(u)) \right) \geq 1 - \beta,$$

$$\text{Prob}^N \left( \mathbb{P}(u) \in \mathcal{M}_{\text{It}}(\mathcal{Z}(u)) \right) = 1,$$

which results in

$$\text{Prob}^N \left( \mathbb{P}(u) \in \mathcal{P}(u) \right) \geq 1 - \beta,$$

with

$$\mathcal{P}(u) := \mathbb{B}_{\epsilon(\beta)}(\hat{\mathbb{P}}(u)) \cap \mathcal{M}_{\text{It}}(\mathcal{Z}(u)).$$

**Step 2: (Certificate of **P1**)** From the previous reasoning, for a given  $u$  we have  $\mathbb{P}(u) \in \mathcal{P}(u)$  with probability at least  $1 - \beta$ . Then, with probability at least  $1 - \beta$  the objective value of **(P1)** satisfies the following

$$\mathbb{E}_{\mathbb{P}(u)} [H(u; \rho)] \geq \inf_{\mathbb{Q} \in \mathcal{P}(u)} \mathbb{E}_{\mathbb{Q}} [H(u; \rho)].$$

Let  $J(u)$  be

$$J(u) := \inf_{\mathbb{Q} \in \mathcal{P}(u)} \mathbb{E}_{\mathbb{Q}} [H(u; \rho)],$$

which results in

$$\text{Prob}^N \left( \mathbb{E}_{\mathbb{P}(u)} [H(u; \rho)] \geq J(u) \right) \geq 1 - \beta.$$

Then the proposed certificate  $J(u)$  of **(P1)** satisfies guarantee **(9)**, which completes the proof.  $\blacksquare$

**Proof of Theorem III.2:** We achieve it by three steps. First, we show that Problem **(P2)** can be equivalently reduced to a finite-dimensional problem. Then we equivalently reformulate the resulting problem into a maximization problem. Finally, we show the performance guarantees of **(P3)**.

**Step 1: (Finite-dimensional reduction of **(P2)**)** We express  $J(u)$  as follows

$$\begin{aligned} J(u) &= \begin{cases} \inf_{\mathbb{Q}} \int_{\mathcal{Z}(u)} H(u; \rho) \mathbb{Q}(d\rho), \\ \text{s. t. } \mathbb{Q} \in \mathcal{M}_{\text{It}}(\mathcal{Z}(u)), d_W(\mathbb{Q}, \hat{\mathbb{P}}(u)) \leq \epsilon(\beta), \end{cases} \\ &= \begin{cases} \inf_{\mathbb{Q}, \Pi} \int_{\mathcal{Z}(u)} H(u; \rho) \mathbb{Q}(d\rho), \\ \text{s. t. } \int_{\mathcal{Z}(u) \times \mathcal{Z}(u)} \|\rho - \rho'\| \Pi(d\rho, d\rho') \leq \epsilon(\beta), \\ \Pi \text{ is a distribution of } \rho \text{ and } \rho' \\ \text{with marginals } \mathbb{Q} \text{ and } \hat{\mathbb{P}}(u) \in \mathcal{M}_{\text{It}}(\mathcal{Z}(u)), \end{cases} \\ &= \begin{cases} \inf_{\mathbb{Q}^{(l)}, l \in \mathcal{L}} \frac{1}{N} \sum_{l \in \mathcal{L}} \int_{\mathcal{Z}(u)} H(u; \rho) \mathbb{Q}^{(l)}(d\rho), \\ \text{s. t. } \frac{1}{N} \sum_{l \in \mathcal{L}} \int_{\mathcal{Z}(u)} \|\rho - \rho^{(l)}\| \mathbb{Q}^{(l)}(d\rho) \leq \epsilon(\beta), \\ \text{(10), } \mathbb{Q}^{(l)} \in \mathcal{M}_{\text{It}}(\mathcal{Z}(u)), \forall l \in \mathcal{L}, \end{cases} \end{aligned}$$

$$= \begin{cases} \inf_{\mathbb{Q}^{(l)}, l \in \mathcal{L}} \sup_{\lambda \geq 0} \frac{1}{N} \sum_{l \in \mathcal{L}} \int_{\mathcal{Z}(u)} H(u; \rho) \mathbb{Q}^{(l)}(d\rho) \\ \quad + \lambda \left( \frac{1}{N} \sum_{l \in \mathcal{L}} \int_{\mathcal{Z}(u)} \|\rho - \rho^{(l)}\| \mathbb{Q}^{(l)}(d\rho) - \epsilon(\beta) \right), \\ \text{s. t. (10), } \mathbb{Q}^{(l)} \in \mathcal{M}_{\text{It}}(\mathcal{Z}(u)), \forall l \in \mathcal{L}, \end{cases}$$

where the first equality applies the definition of the expectation operation; the second equality uses the definition of Wasserstein metric; the third equality exploits the fact that the joint distribution  $\Pi$  can be characterized by the marginal distribution  $\mathbb{P}(u)$  of  $\rho'$  and the conditional distributions  $\mathbb{Q}^{(l)}$  of  $\rho$  given  $\rho' = \rho^{(l)}$ ,  $l \in \mathcal{L}$ , written as

$$\Pi := \frac{1}{N} \sum_{l \in \mathcal{L}} \delta_{\{\rho^{(l)}\}} \otimes \mathbb{Q}^{(l)},$$

where admissible sample trajectories  $\{\rho^{(l)}\}_{l \in \mathcal{L}}$  come from (10) and each conditional distribution  $\mathbb{Q}^{(l)}$  is supported on  $\mathcal{M}_{\text{It}}(\mathcal{Z}(u))$ ; and, on the other hand, the fourth equality applies the Lagrangian representation of the problem.

Then, with an extended version of the strong duality results for the moment problem [63, Lemma 3.4], the order of the inf-sup operator in the resulting representation of  $J(u)$  can be switched, resulting in the following expression

$$J(u) = \begin{cases} \sup_{\lambda \geq 0} \inf_{\mathbb{Q}^{(l)}, l \in \mathcal{L}} -\lambda \epsilon(\beta) \\ \quad + \frac{1}{N} \sum_{l \in \mathcal{L}} \int_{\mathcal{Z}(u)} (\lambda \|\rho - \rho^{(l)}\| + H(u; \rho)) \mathbb{Q}^{(l)}(d\rho), \\ \text{s. t. (10), } \mathbb{Q}^{(l)} \in \mathcal{M}_{\text{It}}(\mathcal{Z}(u)), \forall l \in \mathcal{L}, \end{cases}$$

Move the inf operator into the sum operator, we have

$$J(u) = \begin{cases} \sup_{\lambda \geq 0} -\lambda \epsilon(\beta) \\ \quad + \frac{1}{N} \sum_{l \in \mathcal{L}} \left\{ \inf_{\mathbb{Q}^{(l)} \in \mathcal{M}_{\text{It}}(\mathcal{Z}(u))} \mathbb{E}_{\mathbb{Q}^{(l)}}[\lambda \|\rho - \rho^{(l)}\| + H(u; \rho)] \right\}, \\ \text{s. t. (10).} \end{cases}$$

For each  $l \in \mathcal{L}$ , we claim that

$$\begin{aligned} \inf_{\mathbb{Q}^{(l)} \in \mathcal{M}_{\text{It}}(\mathcal{Z}(u))} \mathbb{E}_{\mathbb{Q}^{(l)}} [\lambda \|\rho - \rho^{(l)}\| + H(u; \rho)] \\ = \inf_{\rho \in \mathcal{Z}(u)} (\lambda \|\rho - \rho^{(l)}\| + H(u; \rho)). \end{aligned}$$

The above claim can be clarified as the following

(a) Let  $p^*$  denote the value of the second term. Then, for any  $\rho \in \mathcal{Z}(u)$ , we have

$$p^* \leq \lambda \|\rho - \rho^{(l)}\| + H(u; \rho),$$

implying

$$p^* \leq \mathbb{E}_{\mathbb{Q}^{(l)}} [\lambda \|\rho - \rho^{(l)}\| + H(u; \rho)],$$

holds for any probability distribution  $\mathbb{Q}^{(l)} \in \mathcal{M}(\mathcal{Z}(u))$ , so does for  $\mathbb{Q}^{(l)} \in \mathcal{M}_{\text{It}}(\mathcal{Z}(u))$ . Therefore, we have

$$p^* \leq \inf_{\mathbb{Q}^{(l)} \in \mathcal{M}_{\text{It}}(\mathcal{Z}(u))} \mathbb{E}_{\mathbb{Q}^{(l)}} [\lambda \|\rho - \rho^{(l)}\| + H(u; \rho)].$$

(b) Next, we claim that the set  $\mathcal{M}_{\text{it}}(\mathcal{Z}(u))$  contains all the Dirac distributions supported on  $\mathcal{Z}(u)$ . Then, for any  $\rho' \in \mathcal{Z}(u)$ , we have

$$\delta_{\{\rho'\}} \in \mathcal{M}_{\text{it}}(\mathcal{Z}(u)),$$

resulting in

$$\begin{aligned} & \inf_{\mathbb{Q}^{(l)} \in \mathcal{M}_{\text{it}}(\mathcal{Z}(u))} \mathbb{E}_{\mathbb{Q}^{(l)}} [\lambda \|\rho - \rho^{(l)}\| + H(u; \rho)] \\ & \leq \lambda \|\rho' - \rho^{(l)}\| + H(u; \rho'), \quad \forall \rho' \in \mathcal{Z}(u), \end{aligned}$$

which implies

$$\inf_{\mathbb{Q}^{(l)} \in \mathcal{M}_{\text{it}}(\mathcal{Z}(u))} \mathbb{E}_{\mathbb{Q}^{(l)}} [\lambda \|\rho - \rho^{(l)}\| + H(u; \rho)] \leq p^*.$$

Therefore, we equivalently write  $J(u)$  as

$$\begin{aligned} J(u) &= \sup_{\lambda \geq 0} -\lambda \epsilon(\beta) + \frac{1}{N} \sum_{l \in \mathcal{L}} \inf_{\rho \in \mathcal{Z}(u)} (\lambda \|\rho - \rho^{(l)}\| + H(u; \rho)), \\ & \text{s. t. (10)}. \end{aligned}$$

Finally, we write Problem **(P2)** as follows

$$\begin{aligned} \text{(P2')} \quad & \sup_{u, \lambda \geq 0} -\lambda \epsilon(\beta) + \frac{1}{N} \sum_{l \in \mathcal{L}} \inf_{\rho \in \mathcal{Z}(u)} (\lambda \|\rho - \rho^{(l)}\| + H(u; \rho)), \\ & \text{s. t. (7), (10)}. \end{aligned}$$

**Step 2: (Equivalent reformulation of (P2'))** Using the definition of the dual norm and moving its sup operator we can write Problem **(P2')** as

$$\begin{aligned} & \sup_{u, \lambda \geq 0} -\lambda \epsilon(\beta) + \frac{1}{N} \sum_{l \in \mathcal{L}} \inf_{\rho \in \mathcal{Z}(u)} \sup_{\|\nu^{(l)}\|_* \leq \lambda} \\ & \quad (\langle \nu^{(l)}, \rho - \rho^{(l)} \rangle + H(u; \rho)), \\ & \text{s. t. (7), (10)}. \end{aligned}$$

Given  $\lambda \geq 0$ , the sets  $\{\nu^{(l)} \in \mathbb{R}^{nT} \mid \|\nu^{(l)}\|_* \leq \lambda\}$  are compact for all  $l \in \mathcal{L}$ . We then apply the minmax theorem between inf and the second sup operators. This results in the switch of the operators, and by combining the two sup operators we have

$$\begin{aligned} & \sup_{u, \lambda, \nu} -\lambda \epsilon(\beta) + \frac{1}{N} \sum_{l \in \mathcal{L}} \inf_{\rho \in \mathcal{Z}(u)} (\langle \nu^{(l)}, \rho - \rho^{(l)} \rangle + H(u; \rho)), \\ & \text{s. t. (7), (10), } \lambda \geq 0, \\ & \quad \|\nu^{(l)}\|_* \leq \lambda, \quad \forall l \in \mathcal{L}. \end{aligned}$$

The objective function can be simplified as follows

$$-\lambda \epsilon(\beta) + \frac{1}{N} \sum_{l \in \mathcal{L}} \langle -\nu^{(l)}, \rho^{(l)} \rangle + \frac{1}{N} \sum_{l \in \mathcal{L}} h^{(l)}(u),$$

where

$$h^{(l)}(u) := \inf_{\rho \in \mathcal{Z}(u)} (\langle \nu^{(l)}, \rho \rangle + H(u; \rho)), \quad \forall l \in \mathcal{L}.$$

For each  $l \in \mathcal{L}$ , we rewrite  $h^{(l)}(u)$  by firstly taking a minus sign out of the inf operator, then exploiting the equivalent representation of sup operation, and finally using the definition of conjugate functions. The function  $h^{(l)}(u)$  results in the following form

$$\begin{aligned} h^{(l)}(u) &= - \sup_{\rho \in \mathcal{Z}(u)} (\langle -\nu^{(l)}, \rho \rangle - H(u; \rho)), \\ &= - \sup_{\rho} (\langle -\nu^{(l)}, \rho \rangle - H(u; \rho) - \chi_{\mathcal{Z}(u)}(\rho)), \\ &= - [H(u; \cdot) + \chi_{\mathcal{Z}(u)}(\cdot)]^* (-\nu^{(l)}). \end{aligned}$$

Further, we apply the property of the inf-convolution operation and push the minus sign back into the inf operator, for each  $h^{(l)}(u)$ ,  $l \in \mathcal{L}$ . The representation of  $h^{(l)}(u)$  results in the following relation

$$\begin{aligned} h^{(l)}(u) &= - \inf_{\mu} ([H(u; \cdot)]^* (-\mu^{(l)} - \nu^{(l)}) \\ &\quad + [\chi_{\mathcal{Z}(u)}(\cdot)]^* (\mu^{(l)})), \\ &= \sup_{\mu} (- [H(u; \cdot)]^* (-\mu^{(l)} - \nu^{(l)}) \\ &\quad - [\chi_{\mathcal{Z}(u)}(\cdot)]^* (\mu^{(l)})). \end{aligned}$$

By substituting  $-\nu^{(l)}$  by  $\nu^{(l)}$ , the resulting optimization problem has the following form

$$\begin{aligned} \sup_{u, \lambda, \mu, \nu} \quad & - \lambda \epsilon(\beta) - \frac{1}{N} \sum_{l \in \mathcal{L}} ([H(u; \cdot)]^* (-\mu^{(l)} + \nu^{(l)}) \\ & + [\chi_{\mathcal{Z}(u)}(\cdot)]^* (\mu^{(l)}) - \langle \nu^{(l)}, \rho^{(l)} \rangle), \\ \text{s. t.} \quad & (7), (10), \lambda \geq 0, \\ & \|\nu^{(l)}\|_{\star} \leq \lambda, \forall l \in \mathcal{L}. \end{aligned}$$

Given  $u$ , the strong duality of linear programs is applicable for the conjugate of the function  $H(u; \cdot)$  and the support function  $\sigma_{\mathcal{Z}(u)}(\mu^{(l)})$ . Using the strong duality and the definition of the support function, we compute, for each  $l \in \mathcal{L}$ , the following

$$[H(u; \cdot)]^* (\nu^{(l)} - \mu^{(l)}) := \begin{cases} 0, & \nu^{(l)} = \mu^{(l)} + \frac{1}{T}u, \\ \infty, & \text{o.w.}, \end{cases}$$

and

$$\begin{aligned} [\chi_{\mathcal{Z}(u)}(\cdot)]^* (\mu^{(l)}) &= \sigma_{\mathcal{Z}(u)}(\mu^{(l)}) \\ &= \begin{cases} \sup_{\xi^{(l)}} \langle \mu^{(l)}, \xi^{(l)} \rangle, \\ \text{s. t.} & 0 \leq \xi_e^{(l)}(t) \leq \rho_e^c(u_e(t)), \forall e \in \mathcal{E}, \forall t \in \mathcal{T}, \end{cases} \\ &= \begin{cases} \inf_{\eta^{(l)}} \sum_{e \in \mathcal{E}, t \in \mathcal{T}} \bar{f}_e \bar{\rho}_e \eta_e^{(l)}(t), \\ \text{s. t.} & [\bar{f} \otimes \mathbf{1}_T + (\bar{\rho} - \rho^c(\bar{u})) \otimes \mathbf{1}_T \circ u] \circ \eta^{(l)} \\ & -\mu^{(l)} \geq \mathbf{0}_{nT}, \\ & \eta^{(l)} \geq \mathbf{0}_{nT}, \end{cases} \end{aligned}$$

We substitute these parts for that in the objective function, take the above inf operator out of a minus sign, and obtain **(P3)**.



Given that all the reformulations in this step hold with equalities, we therefore claim that the above problem is equivalent to **(P2)**. Finally, we claim that the sup operation is indeed achievable, because 1) each component of the variable  $u$  is in a finite set  $\Gamma$  and 2), for any  $u$  that is feasible to the above problem, the above problem with that fixed  $u$  satisfies the Slater's condition, which implies that the above problem is achievable. We therefore claim **(P2)** is equivalent to **(P3)**.

**Step 3: (Performance guarantees of (P3))** Given any feasible point  $(u, \rho, \lambda, \mu, \nu, \eta)$  of **(P3)**, we denote its objective value by  $\hat{J}(u)$ . The value  $\hat{J}(u)$  is a lower bound of **(P3)** and therefore a lower bound for **(P2)**, i.e.,  $\hat{J}(u) \leq J(u)$ . Thus  $\hat{J}(u)$  is an estimate of the certificate for the performance guarantee (9). Therefore,  $(u, \hat{J}(u))$  is a data-driven solution and certificate pair for **(P1)**. ■

**Proof of Lemma IV.1:** The proof follows by the application of the following proposition on each bi-linear term in (13):

**Proposition A.1 (Equivalent reformulation of bi-linear terms [64, Section 2])** *Let  $\mathcal{Y} \subset \mathbb{R}$  be a compact set. Given a binary variable  $x$  and a linear function  $g(y)$  in a continuous variable  $y \in \mathcal{Y}$ ,  $z$  equals the quadratic function  $xg(y)$  if and only if*

$$\begin{aligned} \underline{g}x &\leq z \leq \bar{g}x, \\ g(y) - \bar{g} \cdot (1 - x) &\leq z \leq g(y) - \underline{g} \cdot (1 - x), \end{aligned}$$

where  $\underline{g} = \min_{y \in \mathcal{Y}} \{g(y)\}$  and  $\bar{g} = \max_{y \in \mathcal{Y}} \{g(y)\}$ . □

**Remark A.1 (Regularization technique)** In a later program, we add the following extra constraints to speed up the internal computation of solvers

$$\begin{aligned} \sum_{i \in \mathcal{O}} z_{e,i}^{(l)}(t) &= \eta_e^{(l)}(t), \\ \forall e \in \mathcal{E}, t \in \mathcal{T} \setminus \{0\}, l \in \mathcal{L}, \\ \sum_{i \in \mathcal{O}} y_{e,i}^{(l)}(t) &= \rho_e^{(l)}(t), \\ \forall e \in \mathcal{E}, t \in \mathcal{T} \setminus \{0\}, l \in \mathcal{L}. \end{aligned}$$

These are adapted from the binary representation (11) and the definition of  $y_{e,i}^{(l)}(t)$  and  $z_{e,i}^{(l)}(t)$ . ■

**Proof of Proposition VI.1:** Knowing that  $\rho^* \geq \mathbf{0}_{nTN}$  by constraints (15), we only need to show  $\nu^* \geq \mathbf{0}_{nTN}$ . To prove this, let us assume there exists an optimizer  $\text{sol}^*$  such that, for at least one  $\varepsilon \in \mathcal{E}$ ,  $\tau \in \mathcal{T}$  and  $\ell \in \mathcal{L}$ , it holds  $\nu_\varepsilon^{(\ell),*}(\tau) < 0$ . Then, using constraint (18), we claim  $\mu_\varepsilon^{(\ell),*}(\tau) < 0$ . Next, we show the contradiction to an optimizer by constructing a feasible solution that gives us higher objective value than that resulted from  $\text{sol}^*$ . To achieve this, we perturb variables  $\lambda^*$ ,  $\mu_\varepsilon^{(\ell),*}(\tau)$  and  $\nu_\varepsilon^{(\ell),*}(\tau)$ , and leave other components the same as that in  $\text{sol}^*$ . With such perturbation, only constraints (17), (18), and (19) are varied.

Let  $\text{sol} := (x^*, y^*, z^*, \rho^*, \hat{\lambda}, \hat{\mu}, \hat{\nu}, \eta^*)$  denote the feasible solution we are to construct. We denote by  $\hat{h}^* := \sum_{i \in \mathcal{O}} \gamma^{(i)}(\bar{\rho} - \rho^c(\bar{u})) \otimes \mathbf{1}_T \circ z_i^{(l),*} + \bar{f} \otimes \mathbf{1}_T \circ \eta^{(l),*}$  the unperturbed part in constraint (17) and construct  $\hat{\mu}$  as follows

$$\hat{\mu}_e^{(l)}(t) = \begin{cases} \mu_\varepsilon^{(l),*}(t), & \text{if } (e, t, l) \neq (\varepsilon, \tau, \ell), \\ \min\{\hat{h}_\varepsilon^{(\ell),*}(\tau), -\mu_\varepsilon^{(\ell),*}(\tau)\}, & \text{o.w.} \end{cases}$$

The above construction ensures the feasibility of constraints (17) and furthermore, because  $\hat{h}_\varepsilon^{(\ell),*}(\tau) \geq 0$  and  $\hat{\mu}_\varepsilon^{(\ell),*}(\tau) < 0$ , we claim  $\hat{\mu}_\varepsilon^{(\ell)}(\tau) \geq 0$ . Then let us denote by  $g^* := \frac{1}{T} \sum_{i \in \mathcal{O}} \gamma^{(i)} x_i^*$  the unperturbed part of constraints (18) and construct variable  $\hat{\nu}$  as follows

$$\hat{\nu}_e^{(l)}(t) = \begin{cases} \nu_e^{(l),*}(t), & \text{if } (e, t, l) \neq (\varepsilon, \tau, \ell), \\ \hat{\mu}_\varepsilon^{(\ell)}(\tau) + g_\varepsilon^*(\tau), & \text{o.w.} \end{cases}$$

Again, we have  $\hat{\nu}_\varepsilon^{(\ell)}(\tau) \geq 0$ . Then by letting  $\hat{\lambda} := \max\{\lambda^*, \hat{\nu}_\varepsilon^{(\ell)}(\tau)\}$ , constraints (19) are satisfied. In this way, a feasible solution  $\text{sol}$  is constructed.

Next, we evaluate the difference of the objective values of (P4) resulting from  $\text{sol}$  and  $\text{sol}^*$  in the following

$$\begin{aligned} & \text{objective}(\text{sol}) - \text{objective}(\text{sol}^*) \\ &= \left(-\hat{\lambda} + \lambda^*\right) \epsilon(\beta) + \left(\hat{\nu}_\varepsilon^{(\ell)}(\tau) - \nu_\varepsilon^{(\ell),*}(\tau)\right) \rho_\varepsilon^{(\ell),*}(\tau), \\ &\geq \left(-\hat{\lambda} + \lambda^* + \hat{\nu}_\varepsilon^{(\ell)}(\tau) - \nu_\varepsilon^{(\ell),*}(\tau)\right) \epsilon(\beta), \\ &= \left(\min\{-\lambda^*, -\hat{\nu}_\varepsilon^{(\ell)}(\tau)\} + \lambda^* + \hat{\nu}_\varepsilon^{(\ell)}(\tau)\right) \epsilon(\beta) \\ &\quad - \nu_\varepsilon^{(\ell),*}(\tau) \epsilon(\beta), \\ &> 0, \end{aligned}$$

where the first equality cancels out unperturbed terms; the second inequality applies Assumption VI.1 and the fact that  $\hat{\nu}_\varepsilon^{(\ell)}(\tau) \geq 0$  and  $\nu_\varepsilon^{(\ell),*}(\tau) < 0$ ; the third equality applies construction of  $\hat{\lambda}$ ; and the last inequality is achieved by summing the nonnegative first term and the strict positive second term.

By the above computation, we constructed a feasible solution  $\text{sol}$  with a higher objective value than that of  $\text{sol}^*$ , contradicting the assumption that  $\text{sol}^*$  is an optimizer. ■

**Proof of Lemma VI.1:** Let us denote by (P4'') the Problem (P4) with an extra set of constraints  $\nu \geq \mathbf{0}_{nTN}$ . We prove the lemma in two steps.

**Step 1: (Equivalence of optimizers sets)** First, we use Proposition VI.1 to claim that the set of optimizers of (P4) is the same as that of (P4''). Second, we claim that for any optimizer of (P4'), all the constraints in (23) are active. This means that the set of optimizers of (P4'') are the same as the projection of that of (P4'). Therefore, the optimizers set of (P4) and (P4') are equivalent.

**Step 2: (Performance guarantees)** First, any feasible solution of (P4') correspond to a feasible solution of (P4). This holds because any feasible solution of (P4') satisfies all the constraints of (P4). Next, the objective value of (P4') gives a lower bounds of that of (P4). This can be verified using constraints (23). Finally, the performance guarantees (9) of feasible solution of (P4') can be derived from that of (P4) as in Remark IV.1. ■

**Proof of Lemma VI.2:** We construct  $\bar{\nu}$  by showing boundedness of  $\nu \circ \rho$ . It's known for each  $e \in \mathcal{E}$ ,  $t \in \mathcal{T}$  and  $l \in \mathcal{L}$ , the density  $\rho_e^{(l)}(t)$  is nonnegative and bounded above by  $\max_{e \in \mathcal{E}} \{\bar{\rho}_e\}$ . Then we only need to find the upper bound of  $\nu_e^{(l)}(t)$ . By Assumption IV.1, the variable  $\eta_e^{(l)}(t)$

is bounded. Then computations via constraints (17) and (18) result in upper bound of  $\nu_e^{(l)}(t)$  as the following

$$\begin{aligned} \nu_e^{(l)}(t) &\leq \max_{e \in \mathcal{E}, u_e(t) \in \Gamma} \left\{ (\bar{f}_e + u_e(t)(\bar{\rho}_e - \rho_e^c(\bar{u}_e))) \bar{\eta} + \frac{1}{T} u_e(t) \right\}, \\ &= \max_{e \in \mathcal{E}} \left\{ \bar{u}_e \bar{\rho}_e \bar{\eta} + \frac{1}{T} \bar{u}_e \right\}. \end{aligned}$$

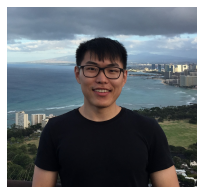
By letting  $\bar{\vartheta} = \sqrt{\max_{e \in \mathcal{E}} \left\{ \bar{u}_e \bar{\rho}_e^2 \bar{\eta} + \frac{1}{T} \bar{u}_e \bar{\rho}_e \right\}}$ , we complete the proof.  $\blacksquare$

## REFERENCES

- [1] D. Aikman, M. Galesic, G. Gigerenzer, S. Kapadia, K. V. Katsikopoulos, A. Kothiyal, E. Murphy, and T. Neumann, "Taking uncertainty seriously: simplicity versus complexity in financial regulation," *Bank of England Financial Stability Paper*, no. 28, 2014.
- [2] S. Thrun, W. Burgard, and D. Fox, *Probabilistic Robotics*, ser. Intelligent Robotics and Autonomous Agents. The MIT Press, 2005.
- [3] N. Dadkhah and B. Mettler, "Survey of motion planning literature in the presence of uncertainty: considerations for UAV guidance," *Journal of Intelligent and Robotic Systems*, vol. 65, no. 1-4, p. 233–246, 2012.
- [4] B. D. Luders, M. Kothari, and J. P. How, "Chance constrained RRT for probabilistic robustness to environmental uncertainty," *AIAA Conf. on Guidance, Navigation and Control*, 2010.
- [5] A. Nilim, L. E. Ghaoui, and V. Duong, "Robust dynamic routing of aircraft under uncertainty," in *Digital Avionics Systems Conference*, vol. 1, 2002, p. 1A5-1 – 1A5-13.
- [6] A. Gray, Y. Gao, T. Lin, K. J. Hedrick, and F. Borrelli, "Stochastic predictive control for semi-autonomous vehicles with an uncertain driver model," in *IEEE Int. Conf. on Intelligent Transportation Systems*, 2013, pp. 2329–2334.
- [7] D. Li, D. Fooladivanda, and S. Martínez, "Data-driven variable speed limit design for highways via distributionally robust optimization," in *European Control Conference*, Napoli, Italy, June 2019, pp. 1055–1061.
- [8] M. Morari and J. H. Lee, "Model predictive control: past, present and future," *Computers & Chemical Engineering*, vol. 23, no. 4-5, pp. 667–682, 1999.
- [9] A. Mesbah, "Stochastic model predictive control: An overview and perspectives for future research," *IEEE Control Systems Magazine*, vol. 36, no. 6, pp. 30–44, 2016.
- [10] D. Mayne, "Robust and stochastic model predictive control: Are we going in the right direction?" *Annual Reviews in Control*, vol. 41, pp. 184–192, 2016.
- [11] J. Rawlings, D. Mayne, and M. Diehl, *Model Predictive Control: Theory, Computation and Design*. Nob Hill Publishing, 2017.
- [12] H. J. Ferreau, H. G. Bock, and M. Diehl, "An online active set strategy to overcome the limitations of explicit mpc," *International Journal on Robust and Nonlinear Control*, vol. 18, no. 8, pp. 816–830, 2008.
- [13] M. Farina, L. Giulioni, and R. Scattolini, "Stochastic linear model predictive control with chance constraints—a review," *Journal of Process Control*, vol. 44, pp. 53–67, 2016.
- [14] M. Prandini, S. Garatti, and J. Lygeros, "A randomized approach to stochastic model predictive control," in *IEEE Int. Conf. on Decision and Control*, 2012, pp. 7315–7320.
- [15] A. Mesbah, S. Streif, R. Findeisen, and R. D. Braatz, "Stochastic nonlinear model predictive control with probabilistic constraints," in *American Control Conference*, 2014, pp. 2413–2419.
- [16] M. A. Sehr and R. R. Bitmead, "Particle model predictive control: Tractable stochastic nonlinear output-feedback mpc," *IFAC Papers Online*, vol. 50, no. 1, pp. 15 361–15 366, 2017.
- [17] J. A. Paulson and A. Mesbah, "An efficient method for stochastic optimal control with joint chance constraints for nonlinear systems," *International Journal on Robust and Nonlinear Control*, vol. 29, no. 15, pp. 5017–5037, 2019.
- [18] L. Magni, G. D. Nicolao, R. Scattolini, and F. Allgöwer, "Robust model predictive control for nonlinear discrete-time systems," *International Journal on Robust and Nonlinear Control*, vol. 13, no. 3-4, pp. 229–246, 2003.
- [19] G. C. Calafiore and L. Fagiano, "Robust model predictive control via scenario optimization," *IEEE Transactions on Automatic Control*, vol. 58, no. 1, pp. 219–224, 2012.
- [20] G. Schildbach, L. Fagiano, C. Frei, and M. Morari, "The scenario approach for stochastic model predictive control with bounds on closed-loop constraint violations," *Automatica*, vol. 50, no. 12, pp. 3009–3018, 2014.
- [21] D. Q. Mayne, E. C. Kerrigan, W. E. Van, and P. Falugi, "Tube-based robust nonlinear model predictive control," *International Journal on Robust and Nonlinear Control*, vol. 21, no. 11, pp. 1341–1353, 2011.
- [22] M. Cannon, B. Kouvaritakis, S. V. Raković, and Q. Cheng, "Stochastic tubes in model predictive control with probabilistic constraints," *IEEE Transactions on Automatic Control*, vol. 56, no. 1, pp. 194–200, 2010.
- [23] D. D. la Penad, A. Bemporad, and T. Alamo, "Stochastic programming applied to model predictive control," in *IEEE Int. Conf. on Decision and Control*, 2005, pp. 1361–1366.
- [24] J. M. Maciejowski, A. L. Visintini, and J. Lygeros, "Nmpc for complex stochastic systems using a markov chain monte carlo approach," in *Assessment and Future Directions of Nonlinear Model Predictive Control*, 2007, pp. 269–281.

- [25] R. Gao and A. Kleywegt, “Distributionally robust stochastic optimization with Wasserstein distance,” *arXiv preprint arXiv:1604.02199*, 2016.
- [26] P. M. Esfahani and D. Kuhn, “Data-driven distributionally robust optimization using the Wasserstein metric: performance guarantees and tractable reformulations,” *Mathematical Programming*, vol. 171, no. 1-2, pp. 115–166, 2018.
- [27] D. Boskos, J. Cortés, and S. Martínez, “Data-driven ambiguity sets with probabilistic guarantees for dynamic processes,” *IEEE Transactions on Automatic Control*, 2020, to appear.
- [28] A. Hakobyan and I. Yang, “Wasserstein distributionally robust motion control for collision avoidance using conditional value-at-risk,” *arXiv preprint arXiv:2001.04727*, 2020, available at <https://arxiv.org/abs/2001.04727>.
- [29] I. Yang, “Wasserstein distributionally robust stochastic control: A data-driven approach,” *IEEE Transactions on Automatic Control*, pp. 1–8, 2020.
- [30] A. Cherukuri and J. Cortés, “Data-driven distributed optimization using Wasserstein ambiguity sets,” in *Allerton Conf. on Communications, Control and Computing*, Monticello, IL, 2017, pp. 38–44.
- [31] —, “Cooperative data-driven distributionally robust optimization,” *IEEE Transactions on Automatic Control*, vol. 65, no. 10, pp. 4400–4407, 2020.
- [32] D. Li and S. Martínez, “Online optimization and data assimilation with performance guarantees,” *IEEE Transactions on Automatic Control*, 2021, to appear. Extended version at arXiv:1901.07377.
- [33] A. A. Kurzhanskiy and P. Varaiya, “Active traffic management on road networks: a macroscopic approach,” *Philosophical Transactions of the Royal Society A*, vol. 368, no. 1928, pp. 4607–4626, 2010.
- [34] S. Jafari and K. Savla, “On structural properties of feedback optimal control of traffic flow under the cell transmission model,” *arXiv preprint arXiv:1805.11271*, 2018.
- [35] A. Jamshidnejad, I. Papamichail, M. Papageorgiou, and B. Schutter, “Sustainable model-predictive control in urban traffic networks: efficient solution based on general smoothing methods,” *IEEE Transactions on Control Systems Technology*, 2017.
- [36] J. Yan and R. R. Bitmead, “Incorporating state estimation into model predictive control and its application to network traffic control,” *Automatica*, vol. 41, no. 4, pp. 595–604, 2005.
- [37] S. Coogan, E. A. Gol, M. Arcak, and C. Belta, “Traffic network control from temporal logic specifications,” *IEEE Transactions on Control of Network Systems*, vol. 3, no. 2, p. 162–172, 2016.
- [38] H. Yu, S. Koga, T. R. Oliveira, and M. Krstic, “Extremum seeking for traffic congestion control with a downstream bottleneck,” *arXiv preprint arXiv:1904.04315*, 2019.
- [39] C. Wu, A. Bayen, and A. Mehta, “Stabilizing traffic with autonomous vehicles,” in *IEEE Int. Conf. on Robotics and Automation*, 2018, pp. 1–7.
- [40] F. Soriguera, I. Martínez, M. Sala, and M. Menéndez, “Effects of low speed limits on freeway traffic flow,” *Transportation Research Part C: Emerging Technologies*, vol. 77, p. 257–274, 2017.
- [41] A. Y. Yazıcıoğlu, M. Roozbehani, and M. A. Dahleh, “Resilient operation of transportation networks via variable speed limits,” in *American Control Conference*, 2017, p. 5623–5628.
- [42] A. Hegyi, B. D. Schutter, and J. Heelendoorn, “MPC-based optimal coordination of variable speed limits to suppress shock waves in freeway traffic,” in *American Control Conference*, vol. 5, 2003, pp. 4083–4088.
- [43] Y. Han, A. Hegyi, Y. Yuan, S. Hoogendoorn, M. Papageorgiou, and C. Roncoli, “Resolving freeway jam waves by discrete first-order model-based predictive control of variable speed limits,” *Transportation Research Part C: Emerging Technologies*, vol. 77, p. 405–420, 2017.
- [44] C. F. Daganzo, “The cell transmission model: A dynamic representation of highway traffic consistent with the hydrodynamic theory,” *Transportation Research Part B: Methodological*, vol. 28, no. 4, p. 269–287, 1994.
- [45] S. Liu, A. Sadowska, J. Frejo, A. Núñez, E. Camacho, H. Hellendoorn, and B. D. Schutter, “Robust receding horizon parameterized control for multi-class freeway networks: A tractable scenario-based approach,” *International Journal on Robust and Nonlinear Control*, vol. 26, no. 6, pp. 1211–1245, 2016.
- [46] D. Work, S. Blandin, O. Tossavainen, B. Piccoli, and A. Bayen, “A traffic model for velocity data assimilation,” *Applied Mathematics Research eXpress (AMRX)*, vol. 2010, no. 1, p. 1–35, 2010.
- [47] J. C. Herrera, D. B. Work, R. Herring, X. J. Ban, Q. Jacobson, and A. M. Bayen, “Evaluation of traffic data obtained via GPS-enabled mobile phones: The Mobile Century field experiment,” *Transportation Research Part C: Emerging Technologies*, vol. 18, no. 4, p. 568–583, 2010.
- [48] M. Van den Berg, A. Hegyi, B. D. Schutter, and J. Hellendoorn, “A macroscopic traffic flow model for integrated control of freeway and urban traffic networks,” in *IEEE Int. Conf. on Decision and Control*, vol. 3, 2003, pp. 2774–2779.
- [49] A. A. Kurzhanskiy and P. Varaiya, “Guaranteed prediction and estimation of the state of a road network,” *Transportation Research Part C: Emerging Technologies*, vol. 21, no. 1, pp. 163–180, 2012.
- [50] C. Daganzo, *Fundamentals of transportation and traffic operations*. Oxford, UK, 1997, vol. 30.
- [51] I. Yperman, “The link transmission model for dynamic network loading,” Ph.D. dissertation, Katholieke Universiteit Leuven, 2007.
- [52] K. Dey, L. Yan, X. Wang, Y. Wang, H. Shen, M. Chowdhury, L. Yu, C. Qiu, and V. Soundararaj, “A review of communication, driver characteristics, and controls aspects of cooperative adaptive cruise control (CACC),” *IEEE Transactions on Intelligent Transportation Systems*, vol. 17, no. 2, pp. 491–509, 2015.
- [53] M. Lighthill and G. Whitham, “On kinematic waves. II. a theory of traffic flow on long crowded roads,” *Royal Society of London. Proceedings Series A: Mathematical, Physical and Engineering Sciences*, vol. 229, no. 1178, p. 317–345, 1955.

- [54] G. Gomes, R. Horowitz, A. A. Kurzhanskiy, P. Varaiya, and J. Kwon, "Behavior of the cell transmission model and effectiveness of ramp metering," *Transportation Research Part C: Emerging Technologies*, vol. 16, no. 4, pp. 485–513, 2008.
- [55] S. Coogan and M. Arcak, "A compartmental model for traffic networks and its dynamical behavior," *IEEE Transactions on Automatic Control*, vol. 60, no. 10, p. 2698–2703, 2015.
- [56] L. V. Kantorovich and G. S. Rubinstein, "On a space of completely additive functions," *Vestnik Leningrad. Univ*, vol. 13, no. 7, p. 52–59, 1958.
- [57] X. Li, A. Tomagard, and P. I. Barton, "Nonconvex generalized Benders decomposition for stochastic separable mixed-integer nonlinear programs," *Journal of Optimization Theory & Applications*, vol. 151, no. 3, p. 425, 2011.
- [58] D. Li and X. Li, "Domain reduction for Benders decomposition based global optimization," *Computers & Chemical Engineering*, vol. 93, pp. 248–265, 2016.
- [59] G. McCormick, "Computability of global solutions to factorable nonconvex programs: Part I—convex underestimating problems," *Mathematical Programming*, vol. 10, no. 1, p. 147–175, 1976.
- [60] D. Li and S. Martínez, "Online data assimilation in distributionally robust optimization," in *IEEE Int. Conf. on Decision and Control*, Miami, FL, USA, December 2018, pp. 1961–1966.
- [61] P. Lopez, M. Behrisch, L. Bieker-Walz, J. Erdmann, Y. Flötteröd, R. Hilbrich, L. Lücken, J. Rummel, P. Wagner, and E. WieBner, "Microscopic traffic simulation using SUMO," in *IEEE Int. Conf. on Intelligent Transportation Systems*, 2018, pp. 2575–2582.
- [62] N. Fournier and A. Guillin, "On the rate of convergence in Wasserstein distance of the empirical measure," *Probability Theory and Related Fields*, vol. 162, no. 3-4, p. 707–738, 2015.
- [63] A. Shapiro, *On duality theory of conic linear problems*. Springer, 2001, p. 135–165.
- [64] F. Glover, "Improved linear integer programming formulations of nonlinear integer problems," *Management Science*, vol. 22, no. 4, p. 455–460, 1975.



**Dan Li** received the B.E. degree in automation from the Zhejiang University, Hangzhou, China, in 2013, the M.Sc. degree in chemical engineering from Queen's University, Kingston, Canada, in 2016. He is currently a Ph.D. student at University of California, San Diego, CA, USA. His current research interests include data-driven systems and optimization, dynamical systems and control, optimization algorithms, applied computational methods, and stochastic systems. He received Outstanding Student Award from Zhejiang University in 2012, Graduate Student Award from Queen's University in 2014, and Fellowship Award from University of California, San Diego, in 2016.



**Dariush Fooladivanda** received the Ph.D. degree from the University of Waterloo, in 2014, and a B.S. degree from the Isfahan University of Technology, all in electrical engineering. He is currently a Postdoctoral Research Associate in the Department of Electrical Engineering and Computer Sciences at the University of California Berkeley. His research interests include theory and applications of control and optimization in large scale dynamical systems.



**Sonia Martínez** is a Professor at the Department of Mechanical and Aerospace Engineering at the University of California, San Diego. She received her Ph.D. degree in Engineering Mathematics from the Universidad Carlos III de Madrid, Spain, in May 2002. Following a year as a Visiting Assistant Professor of Applied Mathematics at the Technical University of Catalonia, Spain, she obtained a Postdoctoral Fulbright Fellowship and held appointments at the Coordinated Science Laboratory of the University of Illinois, Urbana-Champaign during 2004, and at the Center for Control, Dynamical systems and Computation (CCDC) of the University of California, Santa Barbara during 2005.

Her research interests include networked control systems, multi-agent systems, and nonlinear control theory with applications to robotics and cyber-physical systems. For her work on the control of underactuated mechanical systems she received the Best Student Paper award at the 2002 IEEE Conference on Decision and Control. She co-authored with Jorge Cortés and Francesco Bullo "Motion coordination with Distributed Information" for which they received the 2008 Control Systems Magazine Outstanding Paper Award. She is a Senior Editor of the IEEE Transactions on Control of Networked Systems and an IEEE Fellow.